AD-A062 243 TUFTS UNIV MEDFORD MASS DEPT OF PHYSICS F/G 3/2
FINE SCALE RADIO STUDIES OF THE SUN.(U)
OCT 78 K R LANG F19628-76-C-0280
UNCLASSIFIED AFGL -TR-78-0250 NL

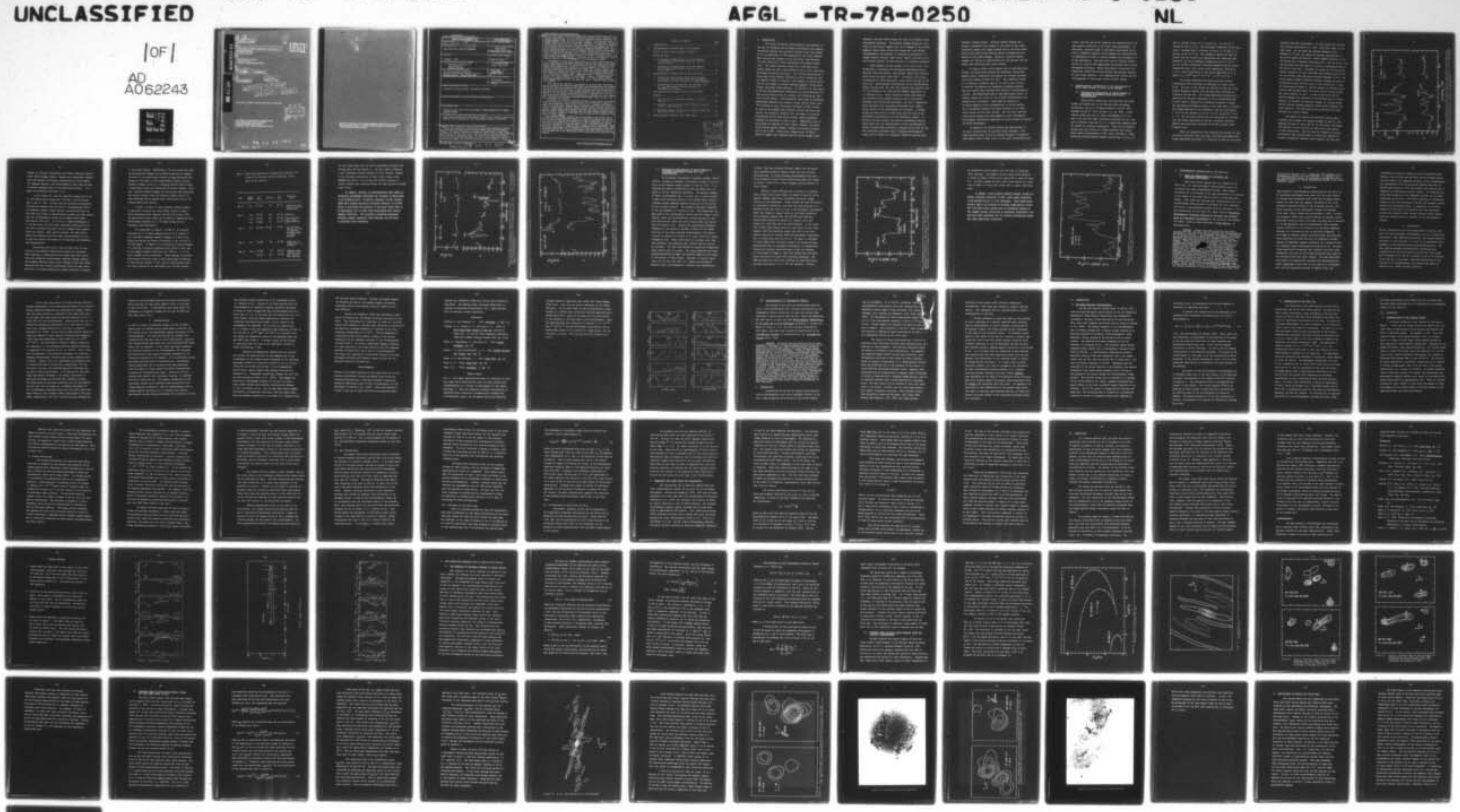

END
DATE FILMED
3 -79
DDC

(18) (19) AFGL-TR-78-0250

(10) NW

LEVEL II

(6) FINE SCALE RADIO STUDIES OF THE SUN.

Kenneth R. Lang

(10)

Department of Physics
Tufts University
Medford, Massachusetts 02155

(9) Final Report.
1 Aug 76 - 1 Oct 78,

(11) 15 Oct 78

(12) 83p.

(15) F19628-76-C-0280

(16) 4643

(17) 03

Approved for public release; distribution unlimited.

AIR FORCE GEOPHYSICS LABORATORY
AIR FORCE SYSTEMS COMMAND
UNITED STATES AIR FORCE
HANSCOM AFB, MASSACHUSETTS 01731

Unclassified

SECURITY CLASSIFICATION OF THIS PAGE (When Data Entered)

REPORT DOCUMENTATION PAGE		READ INSTRUCTIONS BEFORE COMPLETING FORM
1. REPORT NUMBER AFGL-TR-78-0250	2. GOVT ACCESSION NO.	3. RECIPIENT'S CATALOG NUMBER
4. TITLE (and Subtitle) FINE SCALE RADIO STUDIES OF THE SUN		5. TYPE OF REPORT & PERIOD COVERED FINAL REPORT 1 Aug. 1976 - 1 Oct. 1978
		6. PERFORMING ORG. REPORT NUMBER
7. AUTHOR(s) KENNETH R. LANG		8. CONTRACT OR GRANT NUMBER(s) F19628-76-C-0280
9. PERFORMING ORGANIZATION NAME AND ADDRESS Department of Physics Tufts University Medford, MA 02155		10. PROGRAM ELEMENT, PROJECT, TASK AREA & WORK UNIT NUMBERS 62101F, 4643-03-02
11. CONTROLLING OFFICE NAME AND ADDRESS Air Force Geophysics Laboratory Hanscom Air Force Base, Bedford, MA 01731 Contract Monitor: Donald Guidice/PHP		12. REPORT DATE 15 Oct 1976 ? 13. NUMBER OF PAGES 82
14. MONITORING AGENCY NAME & ADDRESS(if different from Controlling Office)		15. SECURITY CLASS. (of this report) Unclassified 15a. DECLASSIFICATION/DOWNGRADING SCHEDULE

16. DISTRIBUTION STATEMENT (of this Report)

Approved for public release, distribution unlimited

17. DISTRIBUTION STATEMENT (of the abstract entered in Block 20, if different from Report)

18. SUPPLEMENTARY NOTES

Portions of this report will be published in Solar Physics and the Astrophysical Journal

19. KEY WORDS (Continue on reverse side if necessary and identify by block number)

Solar Radio Interferometry, Fine Angular Scales, Flare Prediction, Active Sun, Physics of Solar Flares, Quiet Sun, Chromospheric Network, Solar Radio

20. ABSTRACT (Continue on reverse side if necessary and identify by block number)

Major flare eruptions in solar active regions create geophysical disturbances which may seriously disrupt Air Force communication and surveillance systems. This report discusses interferometric observations of solar active regions which show that small-scale, highly circularly polarized sources dominate solar emission at radio wavelengths. The small-scale sources emit intense circularly polarized radiation immediately prior to and during the eruption of solar flares, whereas the circularly polarized emission remains at a lower,

DD FORM 1 JAN 73 1473 EDITION OF 1 NOV 65 IS OBSOLETE

403 317 78 12 13 004

constant level whenever the active regions are quiescent and not erupting. The circular polarization of the flare precursors indicates a direct connection with changing magnetic fields in the solar active regions. The precursors reflect changing magnetic fields which may trigger subsequent flare eruptions, and these trigger sources may serve as reliable flare predictors. Studies of the changes in circularly polarized emission during the flare eruptions suggest that the flare eruption process is also the result of changes in magnetic fields. This report further discusses the synthesis mapping technique in which simultaneous solar observations with as many as 55 different interferometer pairs have been used to produce radio wavelength maps of active regions with second of arc angular resolution. This mapping technique may be used to determine whether the flare trigger sources and the flare eruptions are due to the emergence of new magnetic fields or to the rearrangement of existing magnetic fields.

Observations of solar active regions with two or three element interferometers at centimeter and millimeter wavelengths indicate that solar active regions always exhibit small-scale ($\approx$ 10 seconds of arc), circularly polarized ($\approx$ 40%) sources which dominate solar emission at these wavelengths. As long as the regions are quiescent and not emitting solar flares, the intensity, angular size and degree of circular polarization of these small-scale sources remain remarkably stable for intervals as long as days. It is this stability which allows the construction of synthesis maps. Immediately prior to and during the eruption of solar flares, however, the small-scale sources exhibit dramatic changes in circular polarization of up to 80%. It is these changes which reflect changing magnetic fields, and which may lead to a reliable flare forecasting technique.

When solar active regions are not present on the solar disk, interferometers at centimeter and millimeter wavelengths detect emission from less intense, unpolarized small-scale features which cover the entire solar disk. In this report we also discuss observations of these ubiquitous quiet Sun features which show that they are optically thick thermal radiators with angular sizes of $\approx$ 30 seconds of arc and typical angular separations of $\approx$ 7 minutes of arc. The flux from these sources decreases with increasing radio wavelength, but their temperature increases with increasing wavelength where higher, hotter levels of the solar atmosphere are observed.

This report also contains a detailed discussion of the various instrumental effects which enter into the interpretation of the interferometer signals received when observing a complex source like the Sun. A changing interferometer signal is produced when a complex source is observed near the horizon where the effective interferometer baseline changes rapidly. Baseline induced changes are, however, minimal during source transit (near the local zenith). Moreover these baseline induced changes are associated with 180° phase changes. Signal changes due to intrinsic variations of the small-scale sources can be recognized by the absence of phase changes.

The synthesis mapping technique is also discussed in this report. Two dimensional maps of the small-scale sources in solar active regions are given at two circular polarizations with second of arc angular resolution. For the first time solar active regions have been mapped at radio wavelengths with angular resolutions comparable to those obtained at optical (visible) wavelengths. This means that observations of magnetic field configurations at chromospheric levels (centimeter wavelengths) can be compared with similar observations at the lower lying photospheric levels (optical wavelengths). The final section of this report discusses some of the implications of the reported work for possible future research.

TABLE OF CONTENTS

A. INTRODUCTION

This report discusses interferometric observations of the Sun at centimeter and millimeter wavelengths with angular resolutions between one and fifty seconds of arc (one second of arc is equivalent to 700 kilometers on the solar surface). When sunspots are present on the solar disk, they dominate the solar emission at these wavelengths and angular resolutions. The sunspot emission comes from a few small-scale sources which are only a few seconds of arc in size, and which are highly circularly polarized. The circular polarization of these small-scale features indicates a direct connection with the magnetic fields in sunspots, and changes in circular polarization are thought to reflect emerging magnetic fields which trigger subsequent flare emission. In Section B of this report we discuss interferometric observations of the polarization of small-scale sources prior to, during, and following the emission of solar flares. Interferometric data taken at centimeter wavelengths indicate that sunspots always exhibit small-scale ($\approx$10 seconds of arc), circularly polarized ($\approx$40%) sources. As long as the sunspots are quiescent and not emitting solar flares, the intensity, angular size, and degree of circular polarization of the small-scale sources remain remarkably constant for intervals as long as days. Immediately prior to and during the eruption of solar flares, however, the small-scale sources exhibit dramatic changes in circular polarization of up to 80%. Polarization changes prior to flare emission suggest that changing magnetic fields trigger flare

emission, and that these changes may lead to a reliable flare forecasting technique. Polarization changes during the emission of solar flares suggest that it is changes in the sunspot magnetic fields which provide the energy for solar flares. Interferometric observations of sunspots at millimeter wavelengths exhibit intense, small-scale, highly circularly polarized sources similar to those observed at centimeter wavelengths.

When sunspots are not present on the solar disk, interferometers at centimeter and millimeter wavelengths detect emission from less intense, unpolarized, small-scale features which cover the entire solar disk. In Section C we discuss observations of these ubiquitous, small-scale features of the quiet Sun. Quasi-periodic fluctuations in the interferometer signal indicate that the quiet Sun features have angular sizes of $\lesssim$30 seconds of arc with typical angular separations of $\lesssim$ 7 minutes of arc. These ubiquitous small-scale features are optically thick thermal radiators with a flux which decreases with increasing wavelength, but with a temperature which increases with increasing wavelength where higher, hotter levels of the chromosphere are observed. A thermal origin for the sources is consistent with the lack of any detectable polarization in the interferometer signal. In Section C we also discuss the various instrumental effects which enter into the interpretation of the interferometric signals received when observing a complex source like the Sun. This discussion indicates that a changing interferometer signal can be caused by a changing, effective baseline when

viewing a complex source. Baseline induced changes are, however, associated with changes in the phase of the interferometric signal, and signal changes due to intrinsic variations in the small-scale features can be recognized by the absence of any phase changes. Moreover, baseline induced changes are limited to observations near the horizon, and are absent when observing near source transit.

As long as solar active regions are not emitting solar flares, the small-scale sources are remarkably stable with angular sizes, intensities and degrees of circular polarization which remain constant for days. This stability allows us to construct synthesis maps of the small-scale sources. In Section D we discuss the technique of making synthesis maps and present maps obtained with different interferometric systems. Two-dimensional maps of the small-scale sources in sunspot regions are given at two circular polarizations with second of arc resolution. These maps are expected to delineate magnetic field configurations in active regions, and to eventually pinpoint the exact location of the small-scale sources on the solar surface. For the first time the solar active regions have been mapped at radio wavelengths with angular resolutions comparable to those obtained at optical (visible) wavelengths.

In Section E we briefly discuss the implications of the work reported here for possible future research. The high-resolution maps of active regions obtained at centimeter wavelengths refer to high levels in the solar chromosphere and

corona, and they can now be compared with observations at the same angular resolution in the lower lying photosphere. In particular, synthesis maps at centimeter wavelengths can be used to compare the magnetic field changes and configurations at chromospheric levels to similar changes and configurations in the photosphere. The later data can be obtained simultaneously by using Hα and magnetogram observations with optical wavelength telescopes. These simultaneous observations and comparisons should help decide between the two main theories of solar flare emission - the "emerging flux" theory and the "rearrangement of force-free current fields" theory.

B. INTERFEROMETRIC OBSERVATIONS OF THE POLARIZATION OF SMALL-SCALE SOURCES IN SOLAR ACTIVE REGIONS

1). Polarization Observations of Active Regions at Centimeter Wavelengths using the N.R.A.O. Interferometer

Solar active regions were observed with the three element interferometer at the National Radio Astronomy Observatory, (N.R.A.O.) between November 5 and 10, 1975; November 18 and 22, 1976; and May 10 to 16, 1978. A dual channel system was used at signal wavelengths of 3.7 cm and 11 cm, and both right circularly polarized (R.C.P.) and left circularly polarized (L.C.P.) signals were sampled every 30 seconds at alternate wavelengths. Three 25.9-m diameter paraboloids were placed on a skewed baseline with linear phase center displacements of 600, 1200, and 1800 m. These baselines provided maximum angular resolutions of 12.3, 6.2,

and 4.1 seconds of arc at 3.7 cm and 36.7, 18.3 and 12.2 seconds of arc at 11 cm. The half-power beamwidths of the component antennae were $\approx$ 4 minutes of arc at 3.7 cm and $\approx$ 12 minutes of arc at 11 cm. The parametric amplifiers were bypassed, and the system-noise temperature was completely dominated by the solar brightness temperature of $\approx 2 \times 10^4$ K. For our 30 MHz intermediate frequency bandwidth and 30 second integration time, this system noise temperature resulted in a r.m.s. noise fluctuation in the fringe amplitude of 10 Jy, where 1 Jy = 10^{-23} erg s^{-1} cm^{-2} Hz^{-1} = 10^{-26} W m^{-2} Hz^{-1}.

The fringe amplitudes and phases and the circular polarization were calibrated by observing the radio source 3C 84. The gain of the system was adjusted so that the intermediate frequency signals were the same when observing the calibrator and the Sun. The fringe amplitudes obtained while observing the Sun were calibrated in Jy by multiplying them by GS/A, where G denotes the attenuation required to adjust the intermediate frequency signals to the same level, A denotes the fringe amplitude of the calibrator, and the flux density S of 3C 84 was assumed to be 27.8 Jy at 11 cm and 55.3 Jy at 3.7 cm. The circular polarization was calibrated by assuring that the fringe amplitudes of the two circularly polarized signals were equal when observing 3C 84 with a given interferometer pair.

After the observations were completed we plotted the left circularly polarized (LCP) and right circularly polarized (RCP) fringe amplitudes and phases as a function of time for all three

baselines and both wavelengths. We also plotted the percentage circular polarization V = (LCP - RCP)/(LCP + RCP) at the same times. For any given day between November 5 and November 9 of 1975, the degree of circular polarization of the active region (Mc Math No. 13926) remained constant within 10% during the 12 daylight observing hours. For all wavelengths and baselines used the degree of circular polarization was below 30% for all four days. Although the degree of circular polarization remained low (less than 30%) and constant (within 10%) for the 50-hour observing period between November 5 and 9, the active region suddenly exhibited dramatic changes in circular polarization about one hour prior to the emission of a flare. As illustrated in Figure 1, similar changes in circular polarization were observed about 30 minutes and 15 minutes before the flare emission as well. In view of the fact that no similar changes were observed in the 50 hours prior to flare emission, we believe the observed changes in circular polarization reflect emerging magnetic fields which triggered the flare emission. The implications for predictions of flare emission are clearly evident.

The degree of circular polarization observed while tracking active region 757 between November 18 and 22, 1976 remained constant at about 40% for all five days, and during this period no flare activity was reported by any optical or radio observatory. The fact that no changes in circular polarization were observed when no flares were emitted is valuable statistical evidence which supports the view that

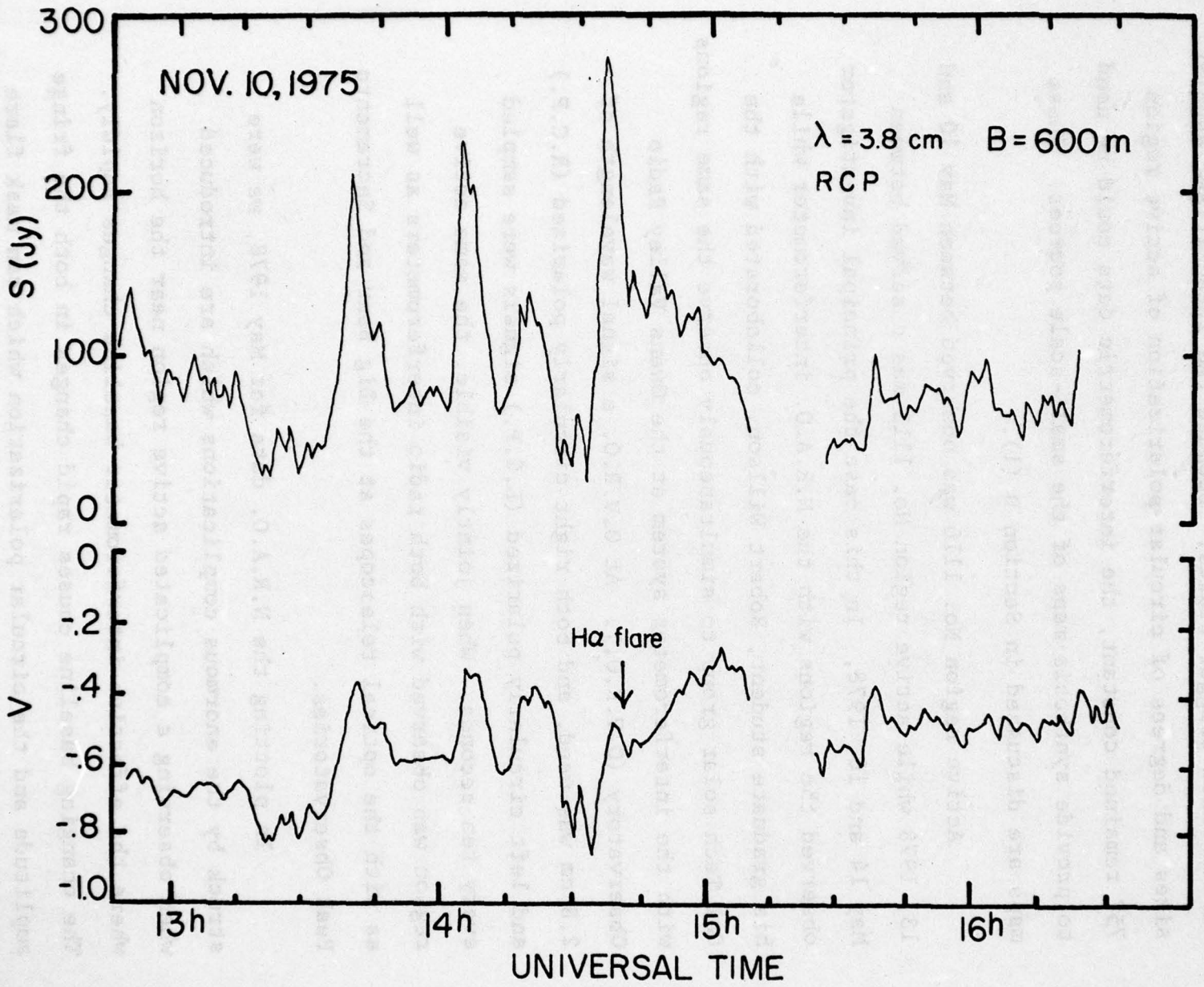

Figure 1. Interferometric observations of an active region (McMath No. 13926) showing large changes in the right circularly polarized (RCP) signal and the degree of circular polarization, V, prior to the eruption of a solar flare (denoted by vertical arrow). Here the observing wavelength is 3.8 cm, the interferometer baseline is 600 m, and the effective angular resolution is 12 seconds of arc.

changes in circular polarization may reflect emerging magnetic fields which trigger flares. Because the intensities, angular sizes and degrees of circular polarization of active region 757 remained constant, the interferometric data could be used to provide synthesis maps of the small-scale sources. Those maps are discussed in Section D (1).

Active region No. 1110 was observed between May 10 and 13, 1978 while active region No. 1112 was observed between May 14 and 16, 1978, In this case the principal investigator observed the regions with the N.R.A.O. interferometer while his graduate student, Robert Willson, collaborated with the Cal Tech solar group to simultaneously observe the same regions with the interferometer system at the Owens Valley Radio Observatory (O.V.R.O.). At O.V.R.O. a signal wavelength of 2.8 cm was used, and both right circularly polarized (R.C.P.) and left circularly polarized (L.C.P.) signals were sampled every ten seconds. When jointly visible, the same active region was observed with both radio interferometers as well as with the optical telescopes at the Big Bear and Sacramento Peak Observatories.

In plotting the N.R.A.O. data for May 1978, we were struck by the enormous complications which are introduced when observing a complicated active region near the horizon where the effective interferometer baseline changes rapidly. The changing baseline causes rapid changes in both the fringe amplitude and the circular polarization which can mask flare emission or circular polarization changes which are intrinsic

to the active region. Nevertheless, the two causes for circular polarization changes can be easily separated, for changes intrinsic to the small-scale sources are not associated with changes in the phase of the interferometer signal, whereas apparent changes induced by a changing baseline when viewing a complicated source are associated with phase changes. Moreover, baseline induced changes are not present when observing near source transit where the baseline changes slowly, or when observing active regions which contain only one or two intense small-scale sources.

In fact, in spite of these baseline induced changes, we were able to detect the solar flares listed in Table 1 while observing active regions 1110 and 1112 in May, 1978. The data given in this table can be used for comparisons with simultaneous observations at the Owens Valley and the Sacramento Peak Observatory.

As illustrated in Figure 2, on May 12 we resolved structure at 3.7 cm whose angular size is $\gtrsim$ 12 seconds of arc, and which undergoes dramatic changes in V which occur before and during the flares illustrated in the top plot of the LCP signal. In Figure 3 we illustrate our second example of a multiple circularly polarized burst which is best seen at the highest angular resolution (B = 1800 m, λ = 3.7 cm and 4 seconds of arc resolution). These changes in circular polarization occurred on May 14 and lasted about 40 minutes. In our previous example of this type of long multiple burst, the flare observed at Hα wavelengths only occurred during

Table 1. Solar flares observed while tracking active region No. 1110 on May 10-13, inclusive, and active region No. 1112 on May 14 to 16, inclusive.

Date	Active Region	U.T. Start	Duration	U.T Peak	Resolution Notes
May 12	1110	$12^h\ 17^m$	5^m	$12^h\ 17^m$	Detected at 3.7cm with all baselines (needs plots).
May 12	1110	$14^h\ 10^m$	10^m	$14^h\ 17^m$	Resolved
	1110	$15^h\ 55^m$	20^m	$15^h\ 57^m$	Only detected at 3.7 cm with 600 m baseline.
	1110	$17^h\ 46^m$	5^m	$17^h\ 47^m$	
May 14	1112	$16^h\ 55^m$, $17^h\ 08^m$,		$17^h\ 25^m$	Multiple burst seen at 3.7 cm at all baselines. Strongest signal at longest baseline.
May 15	1112	$15^h\ 59^m$	10^m	$16^h\ 00^m$	Needs plot of V and I for 11 cm at 1800 m.
May 16	1112	$17^h\ 58^m$	5^m	$18^h\ 01^m$	Resolved, needs plots at 3.7 cm and 11 cm with 600 m baseline.
		$19^h\ 20^m$	40^m	$19^h\ 40^m$	

the last phase after the two radio wavelength precursers had already gone off (see Figure 1). The data shown in Figures 2 and 3 represent further examples in which dramatic changes in the circular polarization of small-scale sources occur immediately prior to and during solar flares; whereas no similar changes were observed during the long intervals between solar flares.

In summary, analysis of interferometric data taken at centimeter wavelengths illustrate the presence of small-scale ($\lesssim$ 10 seconds of arc), circularly polarized ($\gtrsim$ 40%) sources which emit intense circularly polarized emission (up to 80%) prior to and during the eruption of the solar flares seen at Hα wavelengths and at other radio wavelengths with coarser angular resolution. The circularly polarized precursers probably trigger subsequent flare emission and may serve as reliable flare predictors.

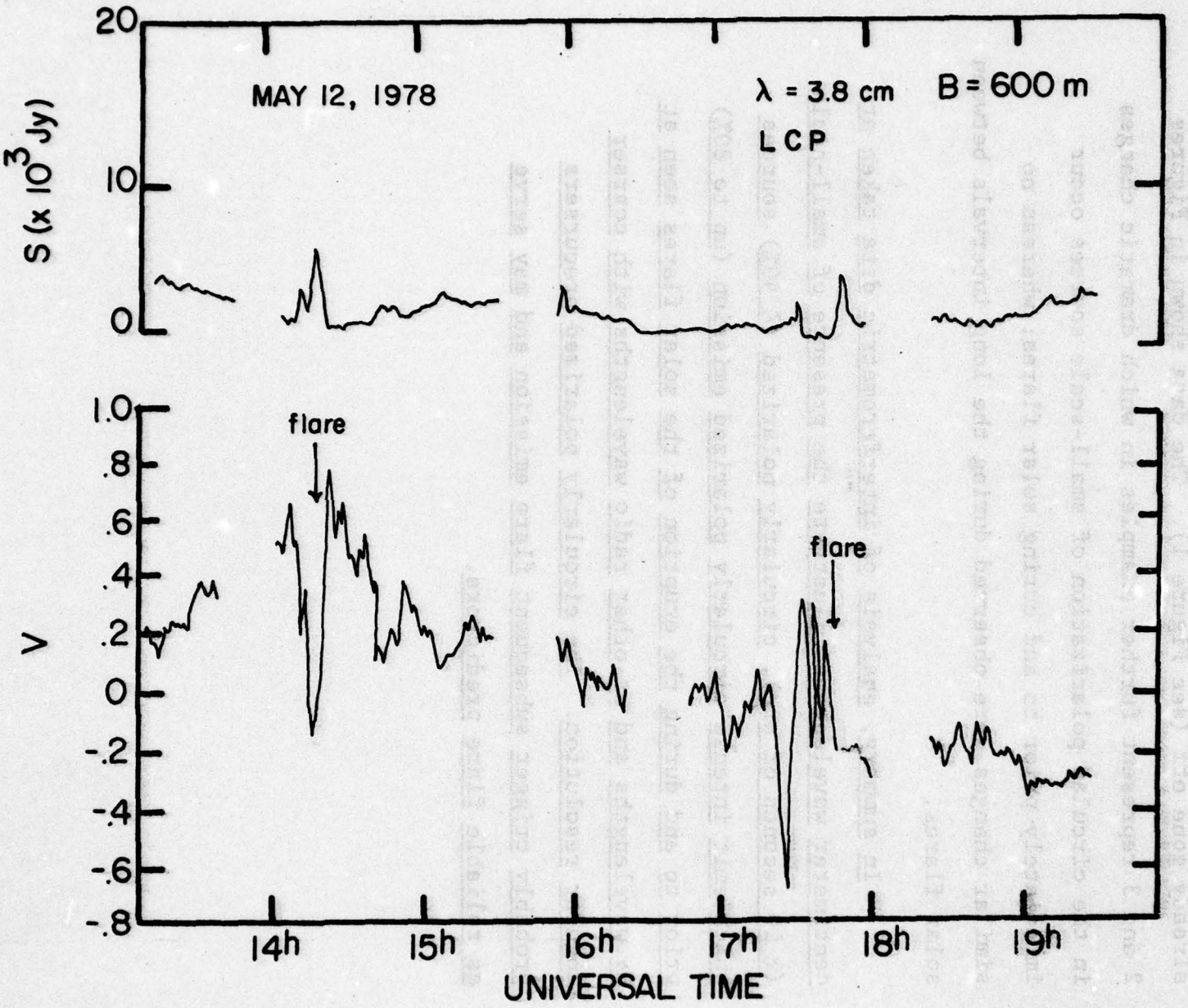

Figure 2. Two examples of interferometric observations of an active region (No. 1110) showing large changes in the degree of circular polarization, V, prior to the emission of solar flares (denoted by vertical arrows). Here, the observing wavelength is 3.8 cm, the interferometer baseline is 600 [illegible] and the effective angular resolution is 12 seconds of arc.

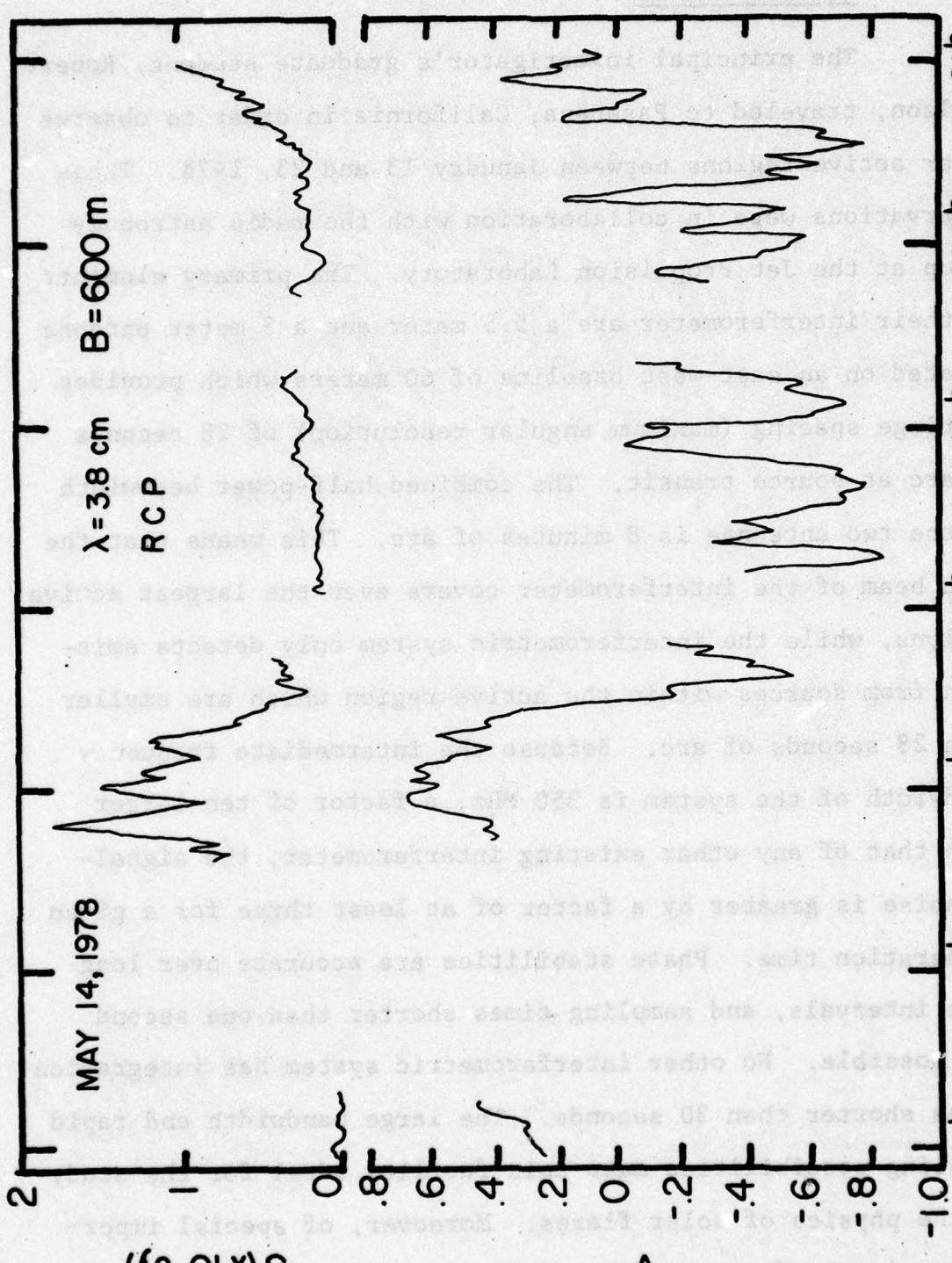

Figure 3. An example of an interferometric observation of a multiple right circularly polarized (RCP) burst lasting about 40 minutes. Here, active region 1112 was observed at a wavelength of 3.8 cm, an interferometer baseline of 1,800 m, and an effective angular resolution of 4 seconds of arc.

2). Polarization Observations of Active Regions at Millimeter Wavelengths using the J.P.L. Interferometer

The principal investigator's graduate student, Robert Willson, traveled to Pasadena, California in order to observe solar active regions between January 13 and 23, 1978. These observations were in collaboration with the radio astronomy group at the Jet Propulsion Laboratory. The primary elements of their interferometer are a 5.5 meter and a 3 meter antenna located on an east-west baseline of 60 meters which provides a fringe spacing (maximum angular resolution) of 28 seconds of arc at source transit. The combined half-power beamwidth of the two antennae is 8 minutes of arc. This means that the main beam of the interferometer covers even the largest active regions, while the interferometric system only detects emission from sources within the active region which are smaller than 28 seconds of arc. Because the intermediate frequency bandwidth of the system is 350 MHz, a factor of ten larger than that of any other existing interferometer, the signal-to-noise is greater by a factor of at least three for a given integration time. Phase stabilities are accurate over long time intervals, and sampling times shorter than one second are possible. No other interferometric system has integration times shorter than 30 seconds. The large bandwidth and rapid sampling possibilities make this facility ideal for the study of the physics of solar flares. Moreover, of special importance, is the fact that the J.P.L. people are willing to dedicate their interferometer to routine solar observations.

In fact, they have obtained internal support for the equipment upgrading needed to measure right and left circular polarizations. No other existing interferometer will ever be available for these routine observations which are needed to collect statistics on flare triggers and the physics of solar flares.

Before we could continue with our plans to systematically obtain active region data, we needed to know if active regions exhibit small-scale circularly polarized trigger sources at 8 mm wavelength. These sources had been discovered at centimeter wavelengths, and there was some question as to whether or not they would be seen at the millimeter wavelengths which see through to deeper levels in the solar atmosphere. Active regions numbered 980, 981 and 985 were therefore respectively observed on January 13, January 18-21 and January 22, 1978 with the 8 mm interferometer. In all cases very intense small-scale structures were found in the active regions with flux densities larger than 1000 Jy and sizes smaller than 28 arc seconds (Note the measurement uncertainty due to system noise was only 30 Jy). In order to determine if these small-scale structures exhibit the strong circular polarization seen at centimeter wavelengths, we mechanically crossed the linearly polarized feeds of the two antennae. As illustrated in Figure 4, this test showed that the small-scale structures are about 40% circularly polarized. The same procedure was used while tracking the quiet Sun and no circular polarization (i.e. $\lesssim$ 5%) was detected. Finally,

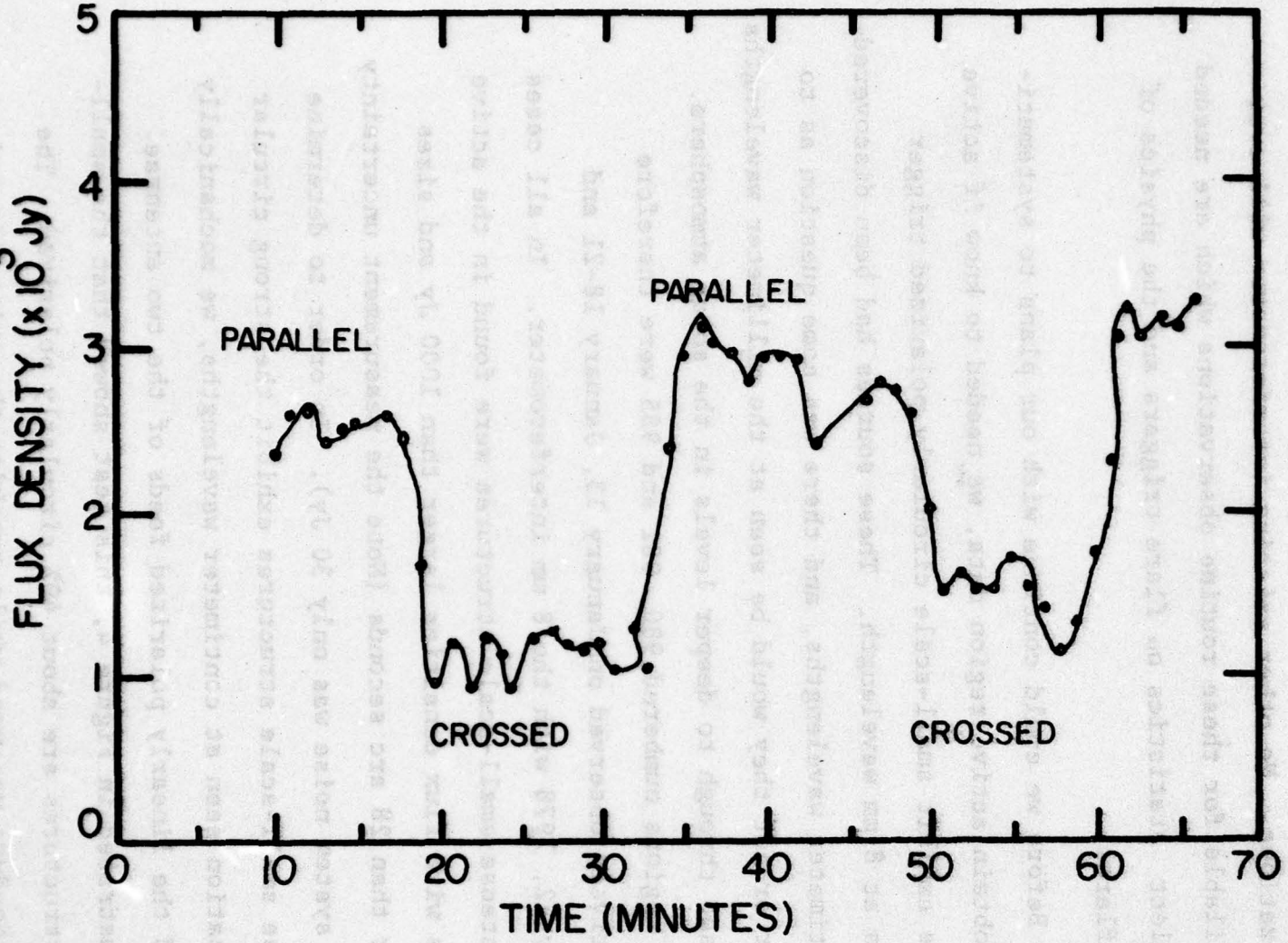

Figure 4. Interferometric observations of a solar active region at 8 mm wavelength and an effective angular resolution of 28 seconds of arc. When the feeds of the two component antennae are crossed, they are only sensitive to circularly polarized radiation. The observations indicate that solar active regions contain small scale ($\lesssim$ 28 seconds of arc) circularly polarized ($\gtrsim$ 40%) sources at 8 mm wavelength.

we tracked the active regions with the hope of detecting flare emission. One example of small-scale flare emission is shown in Figure 5 from active region 980 at about 21 hours U.T. The data suggest multiple small-scale bursts of a duration of about 5 minutes each rather than a single long-lived burst.

In summary, active regions exhibit intense ($\gtrsim$ 1000 Jy), highly circularly polarized ($\gtrsim$ 40%), small-scale structures ($\lesssim$ 28 seconds of arc) at 8 mm wavelength. These small-scale sources seem to be involved in multiple bursts during a flare. The 8 mm small-scale sources must be intimately related to the trigger sources discovered at centimeter wavelengths, and they are ideal candidates for the routine observations needed for flare forecasting statistics.

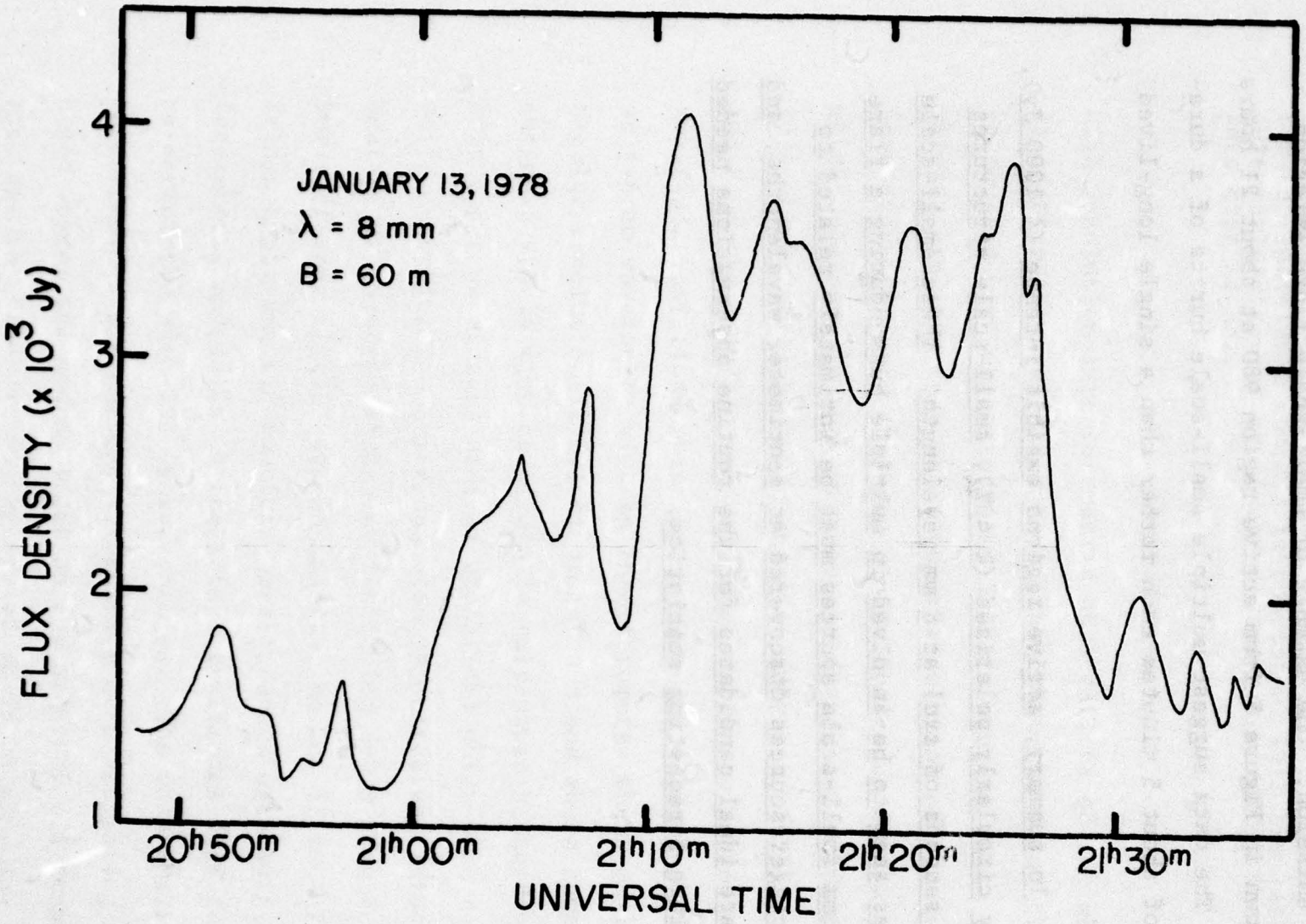

Figure 5. Interferometric observations of a solar flare showing a multiple burst lasting about 20 minutes. Here, the observing wavelength is 8 mm and the effective angular resolution is 28 seconds of arc.

C. INTERFEROMETRIC OBSERVATIONS OF THE QUIET SUN

1). Quiet Sun Observations at Centimeter and Millimeter Wavelengths

When solar active regions were not present on the solar disk, the radio wavelength interferometers were used to observe the solar chromospheric network. Small-scale structures of $\approx$ 30 seconds of arc were discovered to be present at all points of the solar disk at both 11 cm and 8 mm wavelength. These quiet Sun features were observed with the J.P.L. interferometer between March 15 and March 20, 1977, and with the N.R.A.O. interferometer between March 30 and April 4, 1977. The observations are the topic of a paper entitled Ubiquitous Chromospheric Structures Observed in the Quiet Sun at Millimeter and Centimeter Wavelengths by the principal investigator. This paper, which has been published in Solar Physics, is reproduced here.

ABSTRACT. Unique long-term visibility variations are detected when the quiet Sun is observed with interferometers operating at 8 mm and 11 cm wavelength with angular resolutions of 0.5 minutes of arc. Quasi-periodic fluctuations in fringe amplitude are observed with periods between 20 and 30 min., and with amplitude nulls which are correlated with 180° phase changes. These variations are interpreted in terms of a changing projected baseli[illegible]le viewing a few sources with angular sizes of $\approx$0.5 mi[illegible] arc which are distributed within the main interf[illegible]beam with typical angular separations of 7 minu[illegible]of arc. The observed variations cannot be due to expanding or contracting sources of the type envisaged by Bocchia and Poumeyrol (1976) when explaining similar variations observed at 8 mm wavelength. A comparison of the flux observed at 8 mm and 11 cm indicates that the individual sources are optically thick thermal radiators with a flux which decreases with increasing wavelength, but with a temperature which increases with increasing wavelength where higher, hotter levels of the chromosphere are observed. For a source whose angular size is 0.5 minutes of arc, the observed flux values correspond to respective temperatures of 5000 K and

19,000 K at 8 mm and 11 cm -- suggesting that elements of the chromospheric network are being observed. A thermal origin for the individual sources is consistent with the lack of any detectable circular or linear polarization (≤10%) in the interferometer signal.

1. Introduction

High resolution interferometric observations of the quiet Sun at centimeter wavelengths have shown that the solar surface is covered with ubiquitous small-scale sources whose angular extents are less than the angular resolution of the interferometers employed (between 3 and 30 seconds of arc), and which originate in the chromosphere (Kundu and Velusamy, 1974; Lang, 1974a,b; Kundu and Alissandrakis, 1975). Bocchia and Poumeyrol (1976) have called attention to periodic fringe amplitude variations which occur when the quiet Sun is observed at 8.6 mm wavelength with an interferometer whose maximum angular resolution is 0.5 minutes of arc and whose component antennas are 14 minutes of arc in half-power beamwidth. In this paper we discuss similar variations which were detected while observing the quiet Sun with two different interferometers of comparable angular resolution (~0.5 minutes of arc) but different signal wavelengths of 8 mm and 11 cm. Periodic fringe amplitude fluctuations were observed with both interferometers, and nulls in the fringe amplitudes were found to be correlated with 180° phase changes. The peak amplitudes were found to systematically decrease with decreasing hour angle suggesting source sizes on the order of 0.5 minutes of arc, and the fluctuation periods of about 25 min. are

interpreted in terms of changing projected baselines while viewing a few of these sources which are distributed within the main beam of the component antennas of the interferometer. Our interpretation of the variations differs from that of Bocchia and Poumeyrol (1976) who assumed that they are due to expanding or contracting circular sources. By observing the total power detected by the component antennas of our interferometers we are able to show that expanding or contracting sources of the type envisaged by Bocchia and Poumeyrol cannot account for the observed data. A comparison of the flux observed at 8 mm and 11 cm indicates that the individual sources are optically thick thermal radiators whose temperatures are characteristic of elements of the chromospheric network.

2. Observations

We have observed the quet Sun between March 15 and 20, 1977 with the 8 mm wavelength interferometer at the Jet Propulsion Laboratory's Table Mountain Observatory, and between March 30 and April 4, 1977 with the 3.7 cm and 11 cm wavelength interferometer at the National Radio Astronomy Observatory. The main beam and maximum interferometric resolutions were 8 minutes of arc and 28 seconds of arc for the 8 mm system and 12 minutes of arc and 36.7 seconds of arc or 10.5 seconds of arc for the 11 cm system. Detailed descriptions of the 8 mm and 11 cm interferometers are respectively given by Janssen et al. (1978) and Lang (1974a,b).

In all cases the center of the quet Sun was observed. Typical measurements of the amplitude and phase of the observed fringe visibility functions are illustrated in Figure 6 where they have been plotted as a function of the local hour angle. In the upper left hand corner we show one afternoon's observations with the 8 mm interferometer. Similar data were observed during the mornings and afternoons of all five days of observation, and a lengthy discussion of this data is given by Janssen et al. (1978). All of the 8 mm data exhibit variations which are similar to those reported by Bocchia and Poumeyrol (1976) with peak amplitudes of about 5000 Jy (1 Jy = 10^{-26} W m^{-2} Hz^{-1}). As illustrated in Figure 6 similar variations are observed at 11 cm wavelength when the angular resolution is comparable (36.7 minutes of arc, B = 600 m). This is what would be expected if the observed variations are caused by a changing interferometer baseline when viewing complex source structure. Because the r.m.s. measurement uncertainties due to system noise were 30 Jy and 10 Jy, respectively, for the 8 mm and 11 cm data, the observed amplitude variations are not due to noise fluctuations. As illustrated in the lower right hand corner of Figure 6, no similar variations in amplitude and phase are observed when tracking a sunspot. This means that the observed variations are not instrumental, and that they are not caused by a changing orientation of the interferometer sidelobes which view the entire solar disk. Upper limits to this sidelobe effect were placed at 20 Jy and 400 Jy, respectively, for the 11 cm and 8 mm data through the

absence of any detectable amplitude and phase fluctuations while observing the Moon whose angular extent is the same as that of the Sun. In determining these upper limits the difference in brightness between the Sun and the Moon has been taken into account.

3. Interpretations

In order to detect interference fringes the two interferometers must be viewing sources whose angular sizes, ϕ, are ≤ 0.5 minute of arc, the approximate angular resolution of the interferometers. If a few such sources are randomly distributed within the main beam of the interferometer, sinusoidally varying fringe amplitudes with null associated 180° phase shifts will be produced. As the local hour angle increases the effective baseline of the interferometer will decrease and successively lower spatial frequency components of the visibility function will be sampled. If the individual sources are being resolved with $\phi \simeq 0.5$ minutesof arc, sinusoidally varying amplitudes will be observed with peak amplitudes which are small at source transit and which systematically increase with increasing hour angle. Because all of the observed data exhibit this systematic increase, we conclude that $\phi \simeq 0.5$ minutesof arc. The angular separations of the individual sources can be inferred from the period of the fringe amplitude variations. When an interferometer with a maximum angular resolution of 0.5 minutesof arc detects periodically varying fringe amplitudes with a period of 25 min.,

the preferred angular separation of the individual sources is 7 minutes of arc. Because of the flux observed with the interferometers of comparable angular resolution decreases by about an order of magnitude when the wavelength increases from 8 mm to 11 cm, we conclude that the sources are optically thick thermal radiators whose temperatures increase with increasing wavelength where higher, hotter levels of the chromosphere are observed. For a source of angular size ϕ = 0.5 minute of arc and respective flux densities of 5000 Jy and 100 Jy(1 Jy 10^{-23} ergs^{-1} cm^{-2} Hz^{-1}) at 8 mm and 11 cm, the respective temperatures given by the Rayleigh-Jeans law are 5000 K and 19,000 K. A thermal origin for the sources is consistent with the lack of any detectable circular or linear polarization (10%).

Because the temperatures inferred for the individual sources are characteristic of the temperatures of the chromosphere at the heights which correspond to the observing wavelength ($\approx$5000 K at 8 mm and $\approx$ 15,000 K at 11 cm), we conclude that the sources may be part of the chromospheric network whose larger elements have angular sizes of $\gtrsim$0.5 minutes of arc. Independent supporting evidence for this view has been provided by Fürst et al. (1974). They mapped the quiet Sun at wavelengths between 1.25 cm and 6 cm with a large single antenna whose angular resolution was between 0.7 and 2.5 minutes of arc. All of their maps show a random distribution of brightness variations over the entire solar disk with angular separations on the order of 7 minutes of arc

for the most intense features. Because the highest degree of structure was seen at the highest angular resolution, individual sources with angular sizes $\lesssim 0.7$ minute of arc were inferred.

Bocchia and Poumeyrol (1976) have provided an alternative explanation for the unique variations described in this paper. They interpreted the variations in terms of a circular source which expands or contracts with velocities of 10-20 km s^{-1} and which has a maximum diameter of 3 minutes of arc with a brightness temperature of 3×10^4 K. Such an expanding or contracting source would produce a change in the antenna temperature of the component antennae of the interferometers of nearly 1000 K. No antenna temperature changes exceeding 50 K were observed in the signal detected with the component antennae of either the 8 mm or the 11 cm interferometers. This means that expanding or contracting sources of the type envisaged by Bocchia and Poumeyrol cannot account for the observed visibility fluctuations.

Acknowledgments

Several of the ideas presented in this paper grew out of discussions with Michael Janssen and Edward Olsen of the Jet Propulsion Laboratories. They have presented a much more exhaustive additional study of solar interferometry at 8 mm wavelength in Janssen et al. (1978). Radio interferometric studies of the Sun at Tufts University are supported under

Contract No. F19628-76-C-0280 with the Air Force Geophysics Laboratory. The National Radio Astronomy Observatory is operated by Associated Universities, Inc., under contract with the National Science Foundation.

References

Bocchia, R. and Poumeyrol, F.: 1976, Astrophys. J. 204, L107.

Janssen, M. A., Olsen, E. T., and Lang, K. R.: 1978, in Fine Scale Radio Studies of the Sun, Scientific Report No. 1 to the Air Force Geophysic Laboratory (AFGL-TR-77-0208) released January 1978, pp. 10-46.

Fürst, E., Hachenberg, O., and Hirth, W.: 1974, Astron. Astrophys. 36, 123.

Kundu, M. R. and Alissandrakis, C. E.: 1975, Monthly Notices Roy. Astron. Soc. 173, 65.

Kundu, M. R. and Velusamy, T.: 1974, Solar Phys. 34, 125.

Lang, K. R.: 1974a, Solar Phys. 36, 351.

Lang, K. R.: 1974b, Astrophys. J. 192, 777.

Figure Legend

Fig. 6. The signal amplitude and phase as a function of local hour angle while observing the quiet Sun near equinox with interferometers at a variety of wavelengths, λ, and linear baselines, B. Note the apparently periodic fluctuations in amplitude whose intensities systematically increase with increasing hour angle, and the phases which are relatively

constant except at amplitude nulls where 180° phase changes often occur. Also note the faster variations at the longer baselines. In the lower right we show interferometric observations of a sunspot with relatively constant amplitude and a steady phase drift caused by the fact that the radio source is not centered in the main beam of the interferometer. Here the amplitude data are calibrated in Janskies (1 Jy = 10^{-23} erg s^{-1} cm^{-2} Hz^{-1}) and the measurement uncertainties due to system noise alone is 30 Jy and 10 Jy, respectively, for the 8 mm and 11 cm data. The 8 mm data are from Janssen et al. (1977).

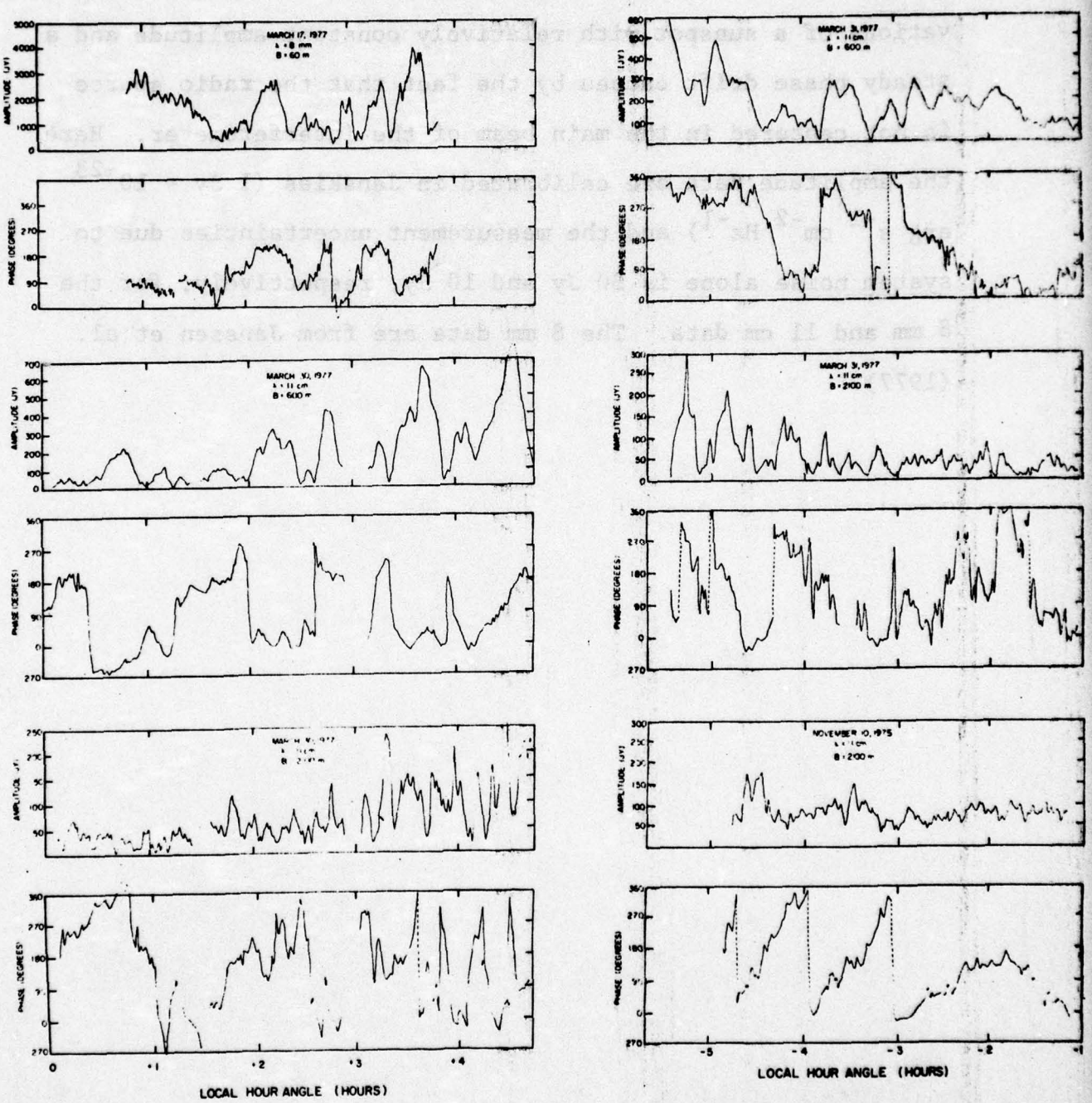
MARCH 17, 1977
λ = 8 mm
B = 60 m
MARCH 31, 1977
λ = 11 cm
B = 600 m
MARCH 31, 1977
λ = 11 cm
B = 2100 m
NOVEMBER 10, 1975
λ = 11 cm
B = 2100 m
AMPLITUDE (μV)
PHASE (DEGREES)
LOCAL HOUR ANGLE (HOURS)

Figure 6

2). Interpretations of Instrumental Effects

One outcome of the quiet Sun observations with the J.P.L. 8 mm interferometer was a serious consideration of the instrumental effects which must be taken into account when observing a complex source like the Sun. These considerations are addressed in a paper entitled Interferometric Observations of the Quiet Sun at 8 mm Wavelength by Michael A. Janssen and Edward T. Olsen at J.P.L. and the principal investigator. This paper, which has been accepted for publication in the Astrophysical Journal, is reproduced here (cf. Astrophysical Journal, March, 1979).

ABSTRACT. The quiet Sun was observed with an interferometer operating at 8.3-mm wavelength and 30 seconds of arc resolution. We find that small-scale brightness structure exists on the Sun which produces a strong, variable signal when observed by an interferometer. Previous observers have obtained similar results at comparable wavelengths and angular resolutions, and it is evident from these and the present results that such small-scale structure is a characteristic feature of the quiet Sun's surface. We conclude from our observations that this structure as seen at 30 seconds of arc resolution is stable or quasi-stable and that the predominant 10-30 minute time variations in our observed signal are caused by changes in the interferometer fringe pattern across this structure. Weaker and more rapid variations may indicate intrinsic time variability in elements of this structure, but the data are contaminated at this level by other instrumental effects. For example, normally occurring antenna pointing variations while observing a greatly extended pattern of sources can plausibly account for these weaker variations. The unambiguous detection of intrinsic time variability is inherently difficult when using a single interferometer at this resolution.

I. INTRODUCTION

Observations of the Sun by typical fixed-baseline radio interferometers would yield negligible results if the Sun's radio brightness were smooth on size scales smaller

than an arc-minute. It is notable, therefore, that several interferometric observations have been reported which show remarkably strong signals (Lang and Zirin, 1973; Kundu and Velusamy, 1974; Bocchia and Poumeyrol, 1974, 1976; Lang, 1978). The wavelengths of these observations ranged from 0.8 to 11 cm, with angular resolutions from 4 to 30 seconds of arc. Strong signals are obtained from quiet as well as active regions. Fine structure in the Sun's radio brightness distribution is implied by these observations and appears to be a ubiquitous feature of the solar disk.

The results of these observations are difficult to interpret since they were obtained using interferometers with only two or three elements. Only partial information about the source is returned in such observations. For example, the reported signals exhibit strong time variations, with fluctuations occurring on time scales of several minutes. Except in special circumstances it is indeterminable whether such time variations are a real property of the source, or result from the observing technique itself. Apparent time variations will be produced when a complex, stable brightness structure is observed with a changing fringe pattern, such as is typically incurred with a fixed baseline on a rotating earth. The same results may be ascribed to real time variations in the source, in which case the source may possess a much simpler brightness structure. Both intrinsic source time variability (Kundu and Velusamy, 1974; Lang, 1974; Bocchia and Poumeyrol, 1974, 1976) and fringe pattern

variations across quasi-stable structure (Kundu and Alissandrakis, 1975) have been invoked to explain existing results. This ambiguity must be resolved before a useful interpretation is possible.

We have attempted to shed some light on this problem by taking advantage of a special condition which pertains when an interferometer is used to observe a source near 0^{o} declination; namely, the fringe pattern becomes stationary at the time of local baseline transit. We observed a quiet region at the center of the Sun for a period of several days around the time of the 1977 vernal equinox, using an interferometer operating at 0.83 cm wavelength and with an east-west baseline giving a maximum angular resolution of 28 seconds of arc. It is evident from the comparison of data obtained near transit with that from large hour angles that the predominent time variability in the observed signal is caused by fringe pattern variations. At a finer level of interpretation, however, the issue is clouded by the likelihood of other instrumentally-induced effects; e.g., normally occurring antenna tracking errors must induce <u>apparent</u> time variations at the edges of the observed source structure. These will produce signal fluctuations indistinguishable from any <u>actual</u> time variations which may occur. We emphasize the importance of such difficulties in the present paper since they apply to previous investigations and must be taken into account in future studies of the fine-scale microwave brightness structure.

II. OBSERVATIONS

A. The Table Mountain Interferometer

The Sun was observed between March 15 and 20, 1977, with the 8-mm wavelength interferometer at the Jet Propulsion Laboratory's Table Mountain Observatory near Wrightwood, California. We give a brief description of this instrument here, and a more complete description will be found in Janssen et al. (1978). The primary elements of the interferometer are a 5.5-meter antenna and a 3-meter antenna located on an east-west baseline of 60 meters (7120 wavelengths), which provides a fringe spacing of 28 seconds of arc at source transit. The combined half-power beamwidth of the two antennas is 18 minutes of arc. The receivers employ double-sideband crystal mixers with an intermediate frequency bandwidth of 350 MHz. A switched-delay compensation network maintains coherence over this bandwidth, with a net random signal loss of less than one percent due to delay error. The local oscillator frequency is 36 GHz. Depending upon the direction of the source relative to the baseline, the natural frequency of the signal varies between 0 and ~1 Hz due to the passage of the source through the interferometer fringe pattern. This natural fringe rate is adjusted to a constant 0.5 Hz by the addition of a small, computer-controlled frequency offset in the local oscillator signal supplied to one receiver. The 0.5 Hz output is integrated for 100 msec and digitized. The resulting data is stacked for a preselected interval to obtain an integrated twenty-point sampling of

the fringe cycle, and analyzed by the on-line computer to determine its amplitude and phase.

In general the response of an interferometer to an extended source brightness distribution $T_B(\eta,\xi)$ may be approximated as

$$V(u,v) = \iint G_1(\eta,\xi)\, G_2^*(\eta,\xi)\, T_B(\eta,\xi)\, e^{i2\pi u\eta} e^{i2\pi v\xi}\, d\eta\, d\xi \qquad (1)$$

(e.g., see Christiansen and Hogbom, 1969). Here u and v are the projections in wavelengths of the baseline on the plane of the sky along the directions of right ascension and declination respectively, and η and ξ are the angular coordinates in these directions. G_1 and G_2 are the complex voltage gains of the respective antennas. The output of the interferometer is thus seen to be the instantaneous Fourier transform, at the spatial frequencies u and v, of the source brightness distribution as modified by the beam patterns of the antennas.

The output of the Table Mountain interferometer for an extended source such as the Sun consists of the amplitude and phase corresponding to the complex visibility function of equation 1. The instrumental phase is unregulated and subject to slow drifts. This rarely exceeds 10°/hour as measured on point sources of known position; nevertheless, the absolute phase of the interferometer is typically unknown. The measured quantity is thus the visibility of equation 1 multiplied by an unknown but effectively constant phase term.

B. Observations of the Quiet Sun

The observations were made during a six-day period around the time of the 1977 vernal equinox. We observed the Sun's center exclusively, which according to the full-disk optical records of Big Bear Solar Observatory was quiet and clear of significant disturbances at the time. The amplitude and phase measurements are shown in Figure 7 as a function of time on each of five days of observation. The data are plotted from contiguous thirty-second integrations of the signal, obtained over continuous intervals varying in duration from 1-1/2 to 4 hours each (in the first interval on March 15 we employed a ten-second integration time). The amplitude is shown in Janskys (1 Jy = 10^{-26} W m $^{-2}$ Hz^{-1}); i.e., an unpolarized point source with a total flux density of 1 Jy would produce a response of unit magnitude. All amplitudes have been corrected for atmospheric attenuation, which amounts to 3% at the zenith. The measurement uncertainty for each 30 sec integration due to system noise alone was in all cases less than 30 Jy, and is negligible on the scale of Figure 7. The measurement error in amplitude was verified to be consistent with the system noise temperature by periodic observations of Venus interspersed with the solar measurements. The flux scale calibration is based on measurements of Venus, which we assumed to be a uniformly bright disk of 460 K with a semidiameter equal to that given by the American Ephemeris and Nautical Almanac. We corrected for its partial resolution by the interferometer (Janssen and Olsen, 1978).

The Venus observations also showed that the residual point-to-point phase uncertainty due to instrumental and atmospheric effects is less than 10°.

III. DISCUSSION

A. Interpretation of the Present Results

We direct attention to two features of the data in Figure 7. First are the strong fluctuations which occur over time scales of approximately 10-30 minutes and dominate the data at large hour angles. For example, we note three such events of about 10-20 minutes duration each, on 17 March from 3 to 4 hours in hour angle, whose regular spacing in this case gives a quasi-periodic appearance. Ignoring for the moment the weaker, more rapid fluctuations, the records beyond about $\pm$ 2 hours from transit give the appearance of a collection of such "events," sometimes overlapping, and varying in amplitude from perhaps 2000 to over 10,000 Jy. The duration of these fluctuations is generally associated with a constant or slowly varying phase, such as in the case of the strong events from -4 to -3 hours on 19 March. In several instances (such as the first record of 15 March) the fluctuations are punctuated by sharply defined nulls which are associated with abrupt phase shifts of approximately 180°. There is a marked grouping of these "events" in that they only appear at large hour angles and are either absent or greatly reduced in peak amplitude within two hours from transit.

Smaller, more rapid fluctuations in both amplitude and phase are seen at all hour angles. These weak fluctuations are most evident around transit where the mean signal is slowly varying, and appear as "noise" with a peak-to-peak amplitude of $\approx$ 1500 Jy superimposed on the data at all hour angles. These fluctuations greatly exceed the actual instrumental noise level of about 30 Jy.

i) Strong Fluctuations

The strong fluctuations are consistent with those which may be produced by the natural time variation of the fringe pattern while observing a fixed distribution of sources. Such an effect has been discussed previously by Kundu and Alissandrakis (1975) and by Lang (1974). The fringe pattern is contained in the exponential terms in the integrand of equation 1, which describe a sinusoidal pattern of fringes of spacing $(u^2 + v^2)^{-1/2}$ whose lines of constant phase are oriented at an angle $\tan^{-1} u/v$ with respect to the direction of increasing right ascension. The projected baseline lengths u and v are shown in Figure 8 for the first and last days of observation. The variation is primarily in the u dimension since the Sun was observed near 0° declination with an east-west baseline. The fringe pattern contracts and expands with very little rotation during the course of a day's observation, remaining nearly constant around transit, and is essentially identical at times equally displaced before and after transit.

The interferometer primarily responds to sources whose dimensions are comparable to or less than the approximately 30 seconds of arc fringe spacing; such sources, however, may be several in number and distributed at random throughout the interferometer's main beam. This beam ($G_1 \times G_2^*$ in equation 1) has a half-power width of 8 minutes of arc for the Table Mountain interferometer. From the Fourier relationship of equation 1, spatial structure distributed through an angular extent $\Delta\eta$ will produce oscillations of typical width w in the transform coordinate $w = (u^2 + v^2)^{1/2}$ as given by $\Delta\eta\,\Delta w \approx 1$. If we consider the observable separation of sources to be limited to the half-power beamwidth, or $\Delta\eta \leq 8$ minutes of arc, then the period of observed fluctuations due to fringe pattern variations is constrained to be $\Delta w/2 \geq 200$. We use $\Delta w/2$ rather than Δw since a typical visibility oscillation will be observed as two separate amplitude fluctuations. For example, a pair of identical point sources separated by an angular distance s gives a sinusoidal visibility function of period $\Delta w = 1/s$, but will be observed as amplitude fluctuations of period $\Delta w/2$ with 180° phase shifts at the nulls.

In Figure 9 we have replotted the data of Figure 7 versus the baseline projection w, rather than hour angle. The pretransit data are shown as solid lines and the post-transit data, where the baseline projection was essentially identical, are drawn over this data as dashed lines. The strong fluctuations beyond ± 2 hours from transit ($w \approx 2000$

to 6000 wavelengths) maintain the same general appearance as in Figure 7, while the weak fluctuations become highly compressed within 2 hours from transit (6000 to 7000 wavelengths). Nevertheless the slow variation of the mean signal around transit in Figure 7 is now seen to produce structure in the range 6000-7000 wavelengths similar to the strong fluctuations at $w < 6000$ wavelengths. These fluctuations over the entire range of baseline projection are consistent with periodicities $\Delta w/2 \geq 200$, and are therefore consistent with a quasi-stable distribution of sources within the main beam of the interferometer.

The dashed curves of Figure 9 would, however, overlay the solid curves if the brightness structure were indeed stable and the observations ideal. The poor correlation may indicate slow time variability in at least some components of the brightness structure. However, we are unable to exclude as a possible cause the systematic variations which would result either from long-term pointing errors, or the slow drift of the Sun through our beam due to solar rotation which we did not take into account in the observation procedure.

Taking brightness structures as the cause of the fluctuations, the largest observed flux peak S_m would be due to constructive interference produced by a number of sources of size $\lesssim$ 30 seconds of arc or less, randomly distributed through the main beam of the interferometer. We may conservatively estimate the average flux per source as

S_m/n, where $n \geq 2$. Taking $S_m = 10^4$ Jy from the largest observed peak on March 19, the average flux per source would consequently be ≤ 5000 Jy. For a source diameter of 30 seconds of arc, the equivalent brightness temperature would be less than 7500 K.

ii) Weak Fluctuations

The weaker, more rapid fluctuations may be ascribed to antenna tracking variations and the fact that we are observing features in a greatly extended source. In an ideal observation of a constant source, the data of Figure 9 would show only smooth variations over scales $\Delta w/2 < 200$ wavelengths. Point-to-point variations caused by instrumental or system noise would be less than 1% of full scale in amplitude and less than 10° in phase. The weak fluctuations show amplitude variations of as much as 1500 Jy, or about 15% of full scale, and would therefore imply time variability in the source. However, pointing variations in the individual antennas will produce an apparent time variability in the extended source, as seen by the interferometer, which can be considerable near the half-power points of the antennas. Short term tracking errors for the individual Table Mountain antennas lie in the range 0.5 to 1 minutes of arc. Such errors permit the measurement of flux from a point source located at the beam center to within 1%; however, signal fluctuations may reach $\pm$ 40% for a source located at the half-power point. As an example, a single point source

contributing 2000 Jy near the half-power point of the interferometer's main beam could account for the observed fluctuations of 1500 Jy in the net signal if the pointing variations of both antennas were occasionally correlated. Apparent phase fluctuations will also be produced by this mechanism. If we are observing a pattern of sources, each of which may contribute as much as 5000 Jy, it is possible that all of the observed weak fluctuations are caused by tracking errors.

Pointing errors naturally occur in the tracking systems of radio antennas, and are typically of magnitudes approaching one-tenth of a beamwidth. This feature would make the observation of small, short-term variations in any greatly extended source exceedingly difficult to verify with existing interferometers. Further, tracking errors may contaminate the measurements over all time scales depending upon the spectrum of these errors. We point out that the usual technique of calibrating the interferometric phase and amplitude on standard point sources is of no help in accounting for these fluctuations.

iii) Influence of the Solar Limb

There is a further possibility that the measurements have been contaminated by the sharp discontinuity of the solar limb even though the limb lies well outside our main beam. Our sidelobes in the range 10 minutes of arc to 16 minutes of arc from the beam center have been measured to possess a more or less uniform gain from 17-20 dB below the central peak.

The transform of a uniformly bright disk as obtained from equation 1 may be approximated by

$$V_{disk}(w) = \sqrt{\frac{8}{\pi}}\,\bar{G}\,S_o(2\,wR)^{-3/2}\cos(2\pi wR - \tfrac{3\pi}{4}) \qquad (2)$$

where the total contributed flux from the disk, $\bar{G}\,S_o$, is the mean sidelobe gain times the total solar flux, S_o, the apparent solar semidiameter is R, and w is the magnitude of the baseline projection. Here we have assumed that $wR >> 1$ (wR varied through the range 12-33 during the course of the observations). Equation 2 predicts peaks in the measured visibility at intervals of $\Delta w \approx 50$. Assuming a Sun brightness temperature of 8700 K and a mean sidelobe gain $\bar{G} = 0.01$, the amplitudes of the peaks computed from equation 2 vary from 120 Jy near transit to as much as 600 Jy near the hour angle limits of the present observations. Although this signal is neither of sufficient amplitude nor of the correct frequency to explain the overall results, the model examined here suggests that some part of the observed weak fluctuations may be due to the solar limb.

iv) An Experimental Check Using the Moon

Conceivably, spurious effects may be generated by the large-scale brightness distribution of the entire Sun as shaped by the beam pattern function $G_1G_2^*$. Other than the solar limb, and the possibility of very strong sources or an occasional strong solar flare in the sidelobes, we can envision no other mechanism which can contribute significantly to the results.

As a general test for such spurious effects, we observed the Moon under the same conditions as we observed the Sun. On April 29, when the Moon's apparent declination passed through 0°, its center was tracked through the hour angle range -4 to 0 hr. No signal exceeding 10 Jy was observed at any time. Since the Sun is approximately 40 times brighter than the Moon at 8 mm, we estimate that if the solar brightness distribution were as uniform as that of the Moon we would have observed a signal less than 400 Jy in the solar observations. Since this is more than an order of magnitude less than that actually observed, we conclude that the only plausible explanation for our results is the presence of small-scale structure on the Sun within the main beam of our interferometer.

B. Comparison with Other Quiet Sun Observations

Our observations can be directly compared with two other interferometric studies of the quiet Sun at millimeter wavelengths. Bocchia and Poumeyrol (1974, 1976) have obtained extensive solar data using the 8 mm interferometer at Bordeaux (Delannoy et al., 1973), the frequency and baseline of which are nearly identical to that of Table Mountain. The Bordeaux interferometer employs smaller antennas and the main beamwidth is approximately 50% greater. Also, Kundu and Velusamy (1974) observed the quiet Sun on several days with the fixed-baseline Hat Creek interferometer (Hills et al., 1973) at a wavelength of 13 mm. The Hat Creek interferometer employed dissimilar antennas yielding an effective beamwidth comparable

to that of the Table Mountain interferometer. The antennas were located on a skewed baseline approximately three times longer measured in units of wavelength. The observations made with these two instruments did not include the special condition of invariant fringes which we obtained around transit. Our results away from transit are similar in appearance to their published data. Bocchia and Poumeyrol note many fluctuations with lobe-like structure, punctuated with nulls associated with 180° phase shifts. The 10-30 minute time scale of their events is comparable to the time scale of events we observed. Since they observed primarily the edge of the Sun their effective beam size containing source structure was more nearly comparable to ours. The Hat Creek data obtained by Kundu and Velusamy are observed to contain periodicities on the order of 5-8 minutes, approximately three times shorter than those we observe.

The typical amplitudes of events in both the Hat Creek and Bordeaux observations are given in terms of antenna temperature, to which we may make comparison by employing the relationship

$$T_A = (A_1 A_2)^{1/2} \frac{S}{2k} \qquad (3)$$

where A_1 and A_2 are the effective aperture areas of the two interferometer elements and S if the source flux. The amplitudes of our events are in the range $T_A \simeq$ 15-25 K, and are well matched by the Bordeaux results, 5 K $\leq T_A \leq$ 10 K, when we account for the difference in antenna sizes. The Hat

Creek amplitudes are in the range 10-15 K for events observed with comparable baseline projections, falling to 5 K at their baseline transit. These amplitudes are somewhat smaller than those we obtain, and the discrepancy may be due to the longer wavelength at which they observed. The striking similarities among these sets of observations lead us to conclude that all three interferometers are observing the same phenomena.

Both Kundu and Velusamy, and Bocchia and Poumeyrol, have interpreted their results as due to time variability of sources of the Sun, hypothesizing that each fluctuation observed corresponds to the brightening of an unresolved or partially resolved region on the Sun. We point out, however, that the period of fluctuations which result from variations in the fringe pattern across a fixed distribution of sources will scale on the average as

$$t \approx (bw)^{-1} \qquad (4)$$

where b is the interferometer main beamwidth and w is the baseline length. The periods observed by Kundu and Velusamy and by Bocchia and Poumeyrol, when scaled by factors of 3 and 1 respectively according to their relative interferometer configurations, are in excellent agreement with the 10-30 minute periods we observe for the strong fluctuations. Therefore, their results are also consistent with an interpretation in terms of quasi-stable source structure.

Lang (1978) observed the quiet Sun at 11 cm wavelength with the NRAO three-element interferometer, making use of two baselines giving resolutions of 36.7 and 10.5 seconds

of arc. The data at the coarser resolution show strong fluctuations comparable to ours, while at the higher resolution the periodicities are indeed increased by a factor of three corresponding to the ratio of the resolutions. These observations also indicate that source structure, rather than intrinsic source time variability, is responsible for the fluctuations, and that the spectrum for the brightness structure extends to the longer wavelengths. The amplitude of the variations observed at the coarser resolution is about 500 Jy, indicating an order of magnitude decrease in flux from 11 cm to 0.8 cm.

Kundu and Alissandrakis (1975) have also considered the difficulty of separating time variability in the radio emission from fluctuations caused by fringe pattern variations. They observed the Sun with the NRAO interferometer under conditions where the fringe pattern was unchanging. They observed at wavelengths of 3.7 and 11 cm wavelength and used baselines varying from 1800 to 56,700 wavelengths. At their shorter baseline spacings (1800 and 5400 wavelengths) they find the observed signal to consist of a large steady component on which a smaller time variable signal is apparent, while at much longer spacings the steady component appears to be much weaker. This time-variable component is similar in its appearance to the weak fluctuations which we ascribe to pointing errors. They did not present data obtained when the fringe pattern was varying to compare with these results.

IV. CONCLUSIONS

It is beyond question that the quiet Sun possesses significant fine structure at the 30 seconds of arc level of angular resolution or smaller; further, the extensive observations of this structure suggest that this brightness structure is an omnipresent feature of the solar radio disk. However, we find that the observational problems posed by radio interferometry of the Sun at $\approx$ 30 seconds of arc resolution are important and that caution must be exercised in interpreting the results. The details of the observed brightness structure and the question of its variability with time remain in doubt due to the inherent limitations in using a single two-element interferometer to examine a greatly extended and complex brightness distribution.

The strong fluctuations which we identify in our data are most plausibly due to stable or quasi-stable fine structure distributed throughout the main beam of our interferometer. The time variability in the interferometer signal must be predominantly due to the changing fringe pattern of the interferometer, since these fluctuations disappear when the fringe pattern becomes stationary around the time of transit.

As a working model we suggest a random distribution of sources $\leq$ 30 seconds of arc in diameter across the solar disk, with the flux contribution from individual sources generally less than 5000 Jy at 8 mm wavelength. We do not exclude the possibility of more complex brightness distributions; e.g., a network of filamentary structures. The

fluctuations observed by others at comparable resolutions and wavelengths are consistent with those we observe, but decrease in amplitude at higher angular resolution (Kundu and Velusamy, 1974; Kundu and Allisandrakis, 1975). Kundu and Velusamy postulate that the sources are uniform in size and shape, and find that the decrease in the amplitude with increasing resolution is consistent with circular sources 9 seconds of arc in diameter. More generally, a distribution of source sizes and shapes would also result in a decrease in amplitude with resolution, and we do not believe a definitive interpretation to be possible with the limited data presently available.

The weaker, more rapid fluctuations which are observed must be caused by a mechanism other than fringe pattern variations since they are not noticeably diminished when the fringe pattern is stationary. Also, the separation of contributing stationary sources which would be implied by these time variations is much larger than the main beamwidth. Such fluctuations, however, would be expected as a consequence of the distributed source structure which gives rise to the strong fluctuations. Virtual time variability in this structure would be induced on the sides of the main beam by normal antenna tracking variations. It therefore becomes impossible to uniquely determine the existence of real time variations in such a case, although these may be present. The same argument applies to the time variations seen by Kundu and Alissandrakis (1975) on their shorter baselines where the variable signal

is much weaker than their steady component. However, the variations seen on their long baselines are relatively stronger than the slow component and are most plausibly interpreted as actual time variability. This higher resolution data may refer to a different set of phenomena (Zirin et al., 1978).

Only a general physical interpretation of these results is possible with the existing data. Comparison with the 11 cm observations (Lang, 1978) indicates a somewhat superthermal spectrum for the observed structure, since the flux from a purely thermal radiator would decrease as λ^{-2} whereas the observed relative decrease is only about λ^{-1}. This is consistent with the presence of optically thick disturbances on an angular scale $\lesssim 30$ seconds of arc which extend to higher, hotter layers of the chromosphere where they are observed at the longer wavelengths, while the radiation mechanism may be due to thermal bremsstrahlung from a hot plasma. The angular scale is consistent with optically observed features on the surface of the Sun such as supergranules, spicule clusters, and elements of the chromospheric network, although we are unable to attempt a particular identification on the basis of the present data.

ACKNOWLEDGMENTS

The Table Mountain interferometer was constructed and is operated under Contract NAS 7-100, sponsored by the National Aeronautics and Space Administration. Radio interferometric studies of the Sun at Tufts University are

supported under Contract No. F19628-76-C-0280 with the Air Force Geophysics Laboratory.

REFERENCES

Bocchia, R., and Poumeyrol, F., 1974, Solar Phys. 38, 193.

Bocchia, R., and Poumeyrol, F., 1976, Ap. J., 204, L. 107.

Christiansen, W.N., and Högbom, J.N., 1969, Radiotelescopes (Cambridge: Cambridge University Press).

Delannoy, J., Lacroix, J., and Blum, E.J., 1973, Proc. Inst. Elec. Electron. Engrs. 61, 1282.

Hills, R.E., Janssen, M.A., Thornton, D.D., and Welch, W.J., 1973, Proc. Inst. Elec. Electron. Engrs. 61, 1278.

Janssen, M.A. and Olsen, E.T., 1978, Icarus 33, 263.

Janssen, M.A., Gary, B.L., Gulkis, S., Olsen, E.T., Soltis, F.S., and Yamane, N.I., 1978, "The Table Mountain 8-mm Wavelength Interferometer," submitted to IEEE Trans. Ant. and Prop.

Kundu, M.R. and Alissandrakis, C.E., 1975, M.N.R.A.S. 173, 65.

Kundu, M.R. and Velusamy, T., 1974, Solar Phys. 34, 125.

Lang, K. R. and Zirin, H., 1973, Bull. A.A.S. 5, 275.

Lang, K. R., 1974, Ap. J. 192, 777.

Lang, K. R., 1978, "Ubiquitous Chromospheric Structures Observed in the Quiet Sun at Millimeter and Centimeter Wavelengths," in press, Solar Physics.

Zirin, H., Hurford, G.J., Marsh, K.A., 1978, Ap. J. 224, in press.

FIGURE CAPTIONS

7. Signal phase and amplitude vs hour angle for all solar data obtained. Universal time and date are indicated for each day. The lines are drawn from data obtained in 30-second integrations (10-sec integrations for the first record of March 15). The phase data possess a 360° ambiguity.

8. Variation of the baseline projections u and v with hour angle. Hour angle is indicated by tick marks and numbers on the curves. The u-v diagrams are shown for the first and last days of observation. The baseline projection is nearly constant in the two-hour period around transit.

9. Signal phase and amplitude vs baseline projection for the data of Figure 7. Pretransit data are shown by solid lines, while the overlapping post-transit data are shown by dashed lines. The slow variations around transit seen in Figure 7 now appear more like the strong fluctuations seen at large hour angles, while the higher frequency and presumably time-dependent components become highly compressed.

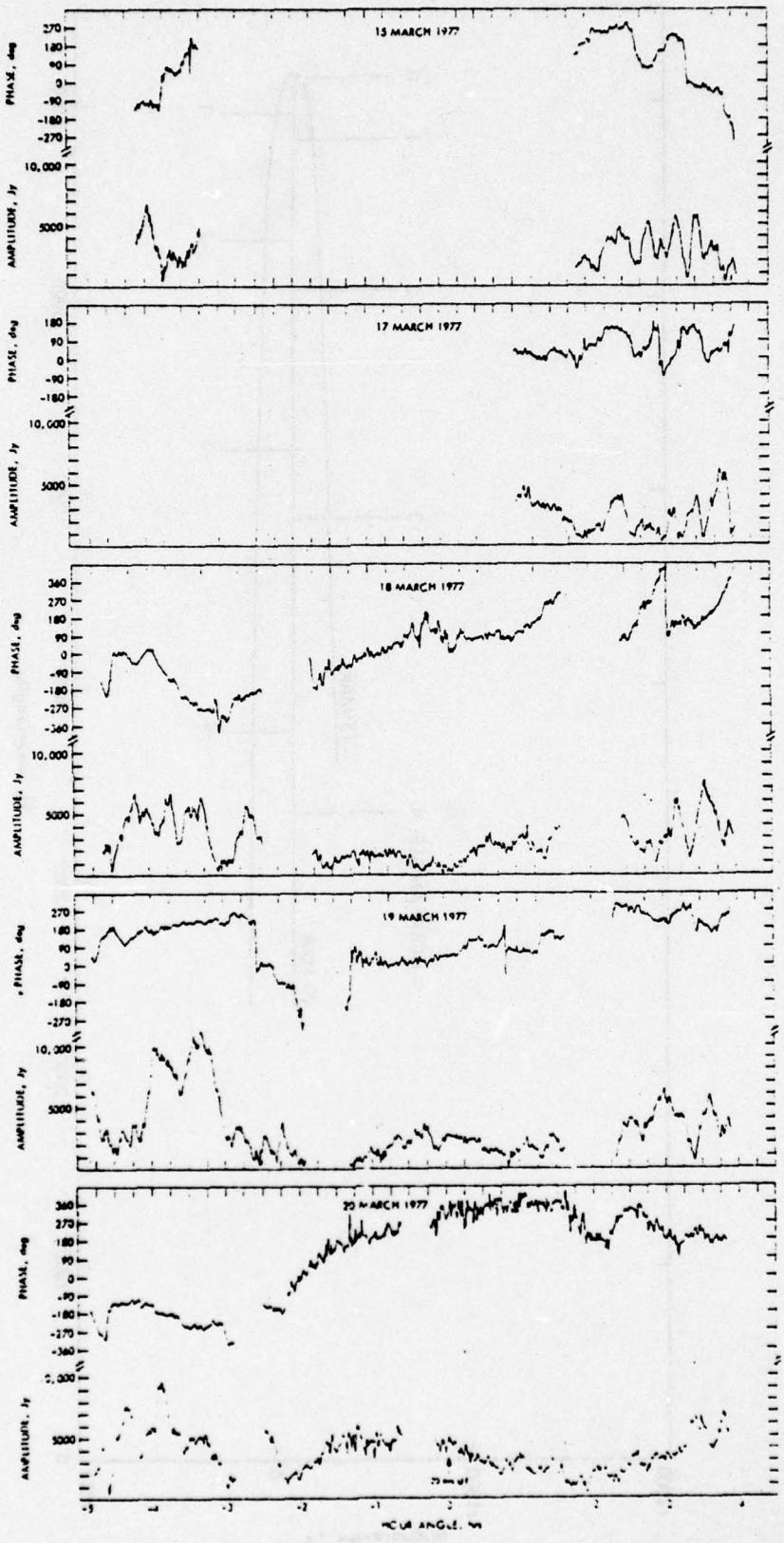

Figure 7 - Janssen, Olsen and Lang

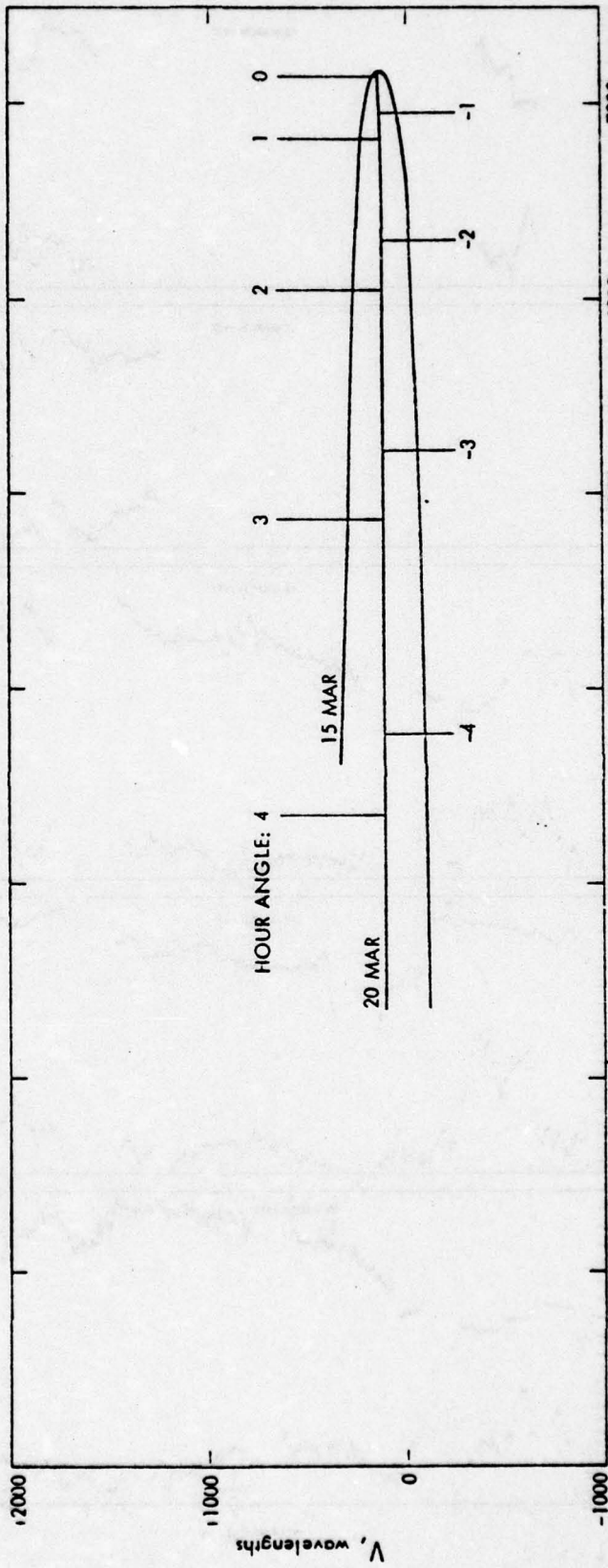

Figure 8 - Janssen, Olsen and Lang

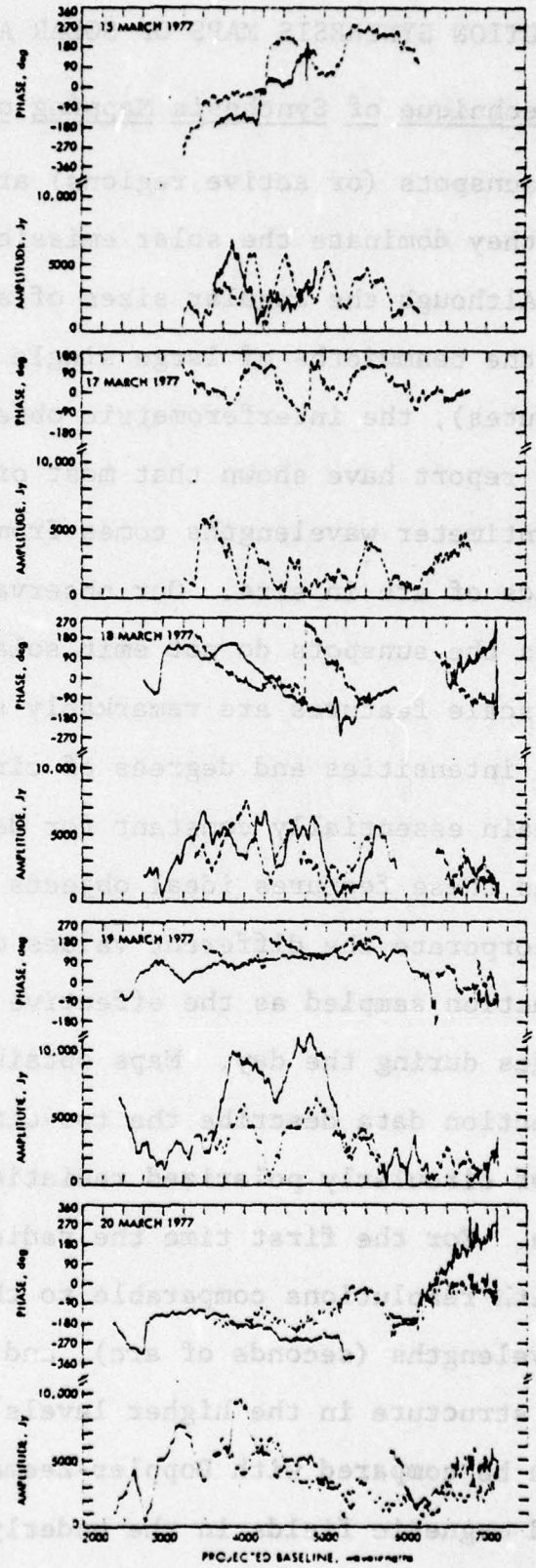

Figure 9 - Janssen, Olsen and Lang

D. HIGH RESOLUTION SYNTHESIS MAPS OF SOLAR ACTIVE REGIONS

1). The Technique of Synthesis Mapping of Active Regions

When sunspots (or active regions) are present on the solar surface they dominate the solar emission at centimeter wavelengths. Although the angular sizes of sunspots are comparable to the beamwidths of large single radio telescopes (a few arc minutes), the interferometric observations discussed in this report have shown that most of the sunspot emission at centimeter wavelengths comes from sources which are only seconds of arc in size. Our observations have shown that as long as the sunspots do not emit solar flares these intense small-scale features are remarkably stable with angular sizes, intensities and degrees of circular polarization which remain essentially constant for days. This stability makes these features ideal objects for synthesis maps which incorporate the different values of the source visibility function sampled as the effective interferometer baseline changes during the day. Maps obtained with the visibility function data describe the two-dimensional spatial distribution of circularly polarized radiation with second of arc resolution. For the first time the radio emission has been mapped with resolutions comparable to those obtainable at optical wavelengths (seconds of arc), and for the first time magnetic structure in the higher levels of the solar atmosphere can be compared with Doppler-Zeeman measurements of motions and magnetic fields in the underlying photosphere.

For each two element interferometer every suitably calibrated measurement of the amplitude and phase of the interferometer signal can be taken as one value of the amplitude and phase of the visibility function, V(u,v). Because corrections for solar rotation and horizontal parallax are incorporated in the computer program which determined the pointing of each antenna, the changing values of the visibility function can be used to measure the brightness distribution of the active region I(x,y), through the fundamental Fourier transform relation

$$V(u,v) = I(x,y)\exp[-2\pi i(ux+vy)]dxdy, \tag{5}$$

where the visibility function and the brightness distribution are determined separately for the two circular polarizations, u and v are the projections of the baseline vector in the direction of increasing right ascension and declination, respectively; and x and y are, respectively, coordinates in the direction parallel to increasing right ascension and declination. These quantities, defined in radians, are given by

$$u = \frac{B}{\lambda}\,[\cos\,\delta_b \sin\,(\mathrm{LHA} - \mathrm{BHA})]$$

$$v = \frac{B}{\lambda}\,[\sin\,\delta_b \cos\,\delta_s - \cos\,\delta_b \sin\,\delta_s \cos\,(\mathrm{LHA} - \mathrm{BHA})], \tag{6}$$

where δ_b and δ_s are the declination of the baseline vector and of the source, respectively, LHA and BHA are the local hour angle of the source and the baseline, and B and λ are

the magnitude of the baseline vector, and the wavelength of observation. The baseline declination and hour angle depend on the geocentric components, B_x, B_y, and B_z of the baseline vector, for each antenna pair.

$$\delta_b = \text{Arctan}\left[\frac{B_z}{(B_x^2 + B_y^2)^{\frac{1}{2}}}\right] \tag{7}$$

$$\text{BHA} = \text{Arctan}\left(\frac{B_y}{B_x}\right). \tag{8}$$

As the earth rotates, and the local hour angle of the source changes, the projected baseline describes an ellipse in the uv plane. The ellipse is centered at $u = 0$, $v = \frac{B}{\lambda} \sin \delta_b \cos \delta_s$, has eccentricity $\cos \delta_s$ and semimajor axis equal to equatorial component of the baseline. If the u-v plane were sufficiently sampled then one could take the inverse transform of equation (5) to obtain the brightness distribution. If the source had a maximum angular extent Δx and Δy in right ascension and declination, then one need only make observations at intervals of $u \sim \frac{1}{\Delta x}$ and $v \sim \frac{1}{\Delta y}$, to obtain a unique map of the source. Since the source brightness is a real function, it follows from equation (5), that $V(u,v) = V^*(-u,-v)$, so we need only measure $V(u,v)$ on one half of the u-v plane. In practice, however, there are never enough interferometer pairs to satisfy the sampling criterion, and so one must resort to using some other technique for obtaining a map.

The procedure we have implemented involves a direct synthesis of a "dirty" map

$$D(x,y) = \frac{1}{N} \sum A_i \cos \phi_i + 2\pi(ux + vy), \qquad (9)$$

where A_i and ϕ_i are the amplitude and phase of observation i, N is the number of observations, and x and y are positions located on a grid of coordinates of the sky. Since the visibility function is symmetric, only the real (cosine) part of the transform need be calculated. The dirty map is the convolution of the true brightness distribution with the response function of a point source. This response function or "dirty beam" is the Fourier transform of the sampling function and is given by

$$B(x,y) = \frac{1}{N} \sum \cos (u_i x + v_i y) w_i, \qquad (10)$$

where w_i is the weight given to each data point.

A deconvolution is then performed by means of the "clean" procedure in which the brightness distribution is decomposed into a sum of beam patterns. The dirty map is searched for the maximum and a point source is fit to the map at that point

$$\text{Amp} = \frac{\sum_{j=1}^{n} \sum_{j=1}^{m} \frac{D_{ij}}{B_{ij}} (B_{ij})^2}{\sum_{j=1}^{n} \sum_{i=1}^{m} B_{ij}^2} . \qquad (11)$$

Here i and j correspond to positions on the grid, which contained 40 by 40 points for our program.

The dirty map usually has a number of disturbing sidelobes caused by insufficient sampling, but if we find that it is identical in every detail to the dirty beam then we know that the brightness distribution consists of a point source at the position of the maximum on the map. If this dirty beam pattern is then subtracted from the dirty map then there should be nothing left. If a "clean" beam pattern, i.e., the ideal main beam of a similar shape but without the sidelobes, is returned to the position, then the result will be the same as that which would have been obtained with normal synthesis if the relevant region in the u-v plane had been observed. Normally the point source response multiplied by some small fraction of Amp, (usually between .2 and .5) centered on the maximum in the map is subtracted from the dirty map. This procedure is repeated a large number of times until all of the significant noise is removed from the map.

2). Synthesis Maps of Solar Active Regions using the N.R.A.O. Interferometer

We have observed the sunspot region 757 with the three element interferometer of the National Radio Astronomy Observatory (N.R.A.O.) between November 18 and 22, 1976. During this period the sunspot travelled from the limb of the Sun to its center and during this period no flare activity was reported by any optical or radio observatory. Observations were taken with a dual channel system at signal frequencies of

2695 MHz (λ = 11 cm) and 8085 MHz (λ = 3.7 cm) with circularly polarized feeds and an intermediate frequency bandwidth of 30 MHz. The 10^4 K signal from the Sun dominated the system noise and gave an r.m.s. noise error in fringe amplitude of 10 Jy (1 Jy = 10^{-23} erg s^{-1} cm^{-2} Hz^{-1}) for our integration time of 30 seconds. Both fringe amplitude and phase were sampled every 30 seconds at alternate signal frequencies, and this data has been used to construct maps of the sunspot regions. Figure 10 shows the u-v tracks for the three baseline configurations and for the observing wavelength of 11 cm on November 22, whereas Figure 11 shows the dirty beam pattern at the same wavelength obtained using the procedures described in the previous section with uniform weighting $w_i = 1$. The half power width is 4 seconds of arc by 20 seconds of arc and the highest sidelobe is 20% of the maximum response.

In Figures 12 and 13 we present high resolution maps of a sunspot region taken at 11 cm wavelength with right and left hand circular polarizations on November 20 and 22, 1976. The structure is extended in the east-west direction where the beam pattern provides maximum resolution. North is in the upward direction, east is to the left, and the length of the arrows denoting direction correspond to 3 seconds of arc. The contours are surface brightness in units of Jansky per square arc second with a maximum value of about eight. The total correlated flux was about 1,000 Jy on November 20 and about 400 Jy on November 22.

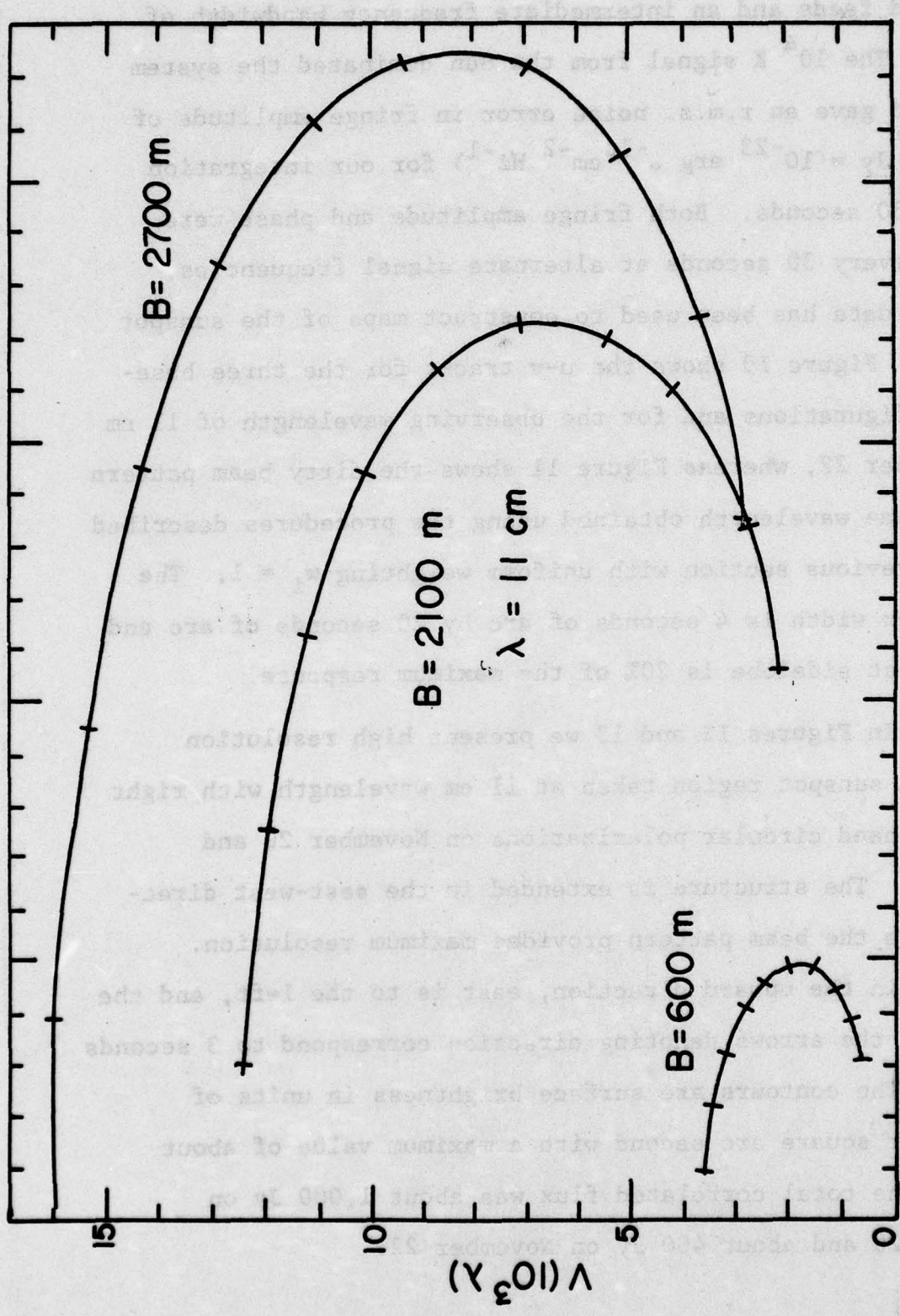

Figure 10. The u-v tracks for the three baselines, B, of the N.R.A.O. interferometer at a wavelength of 11 cm on November 22, 1976.

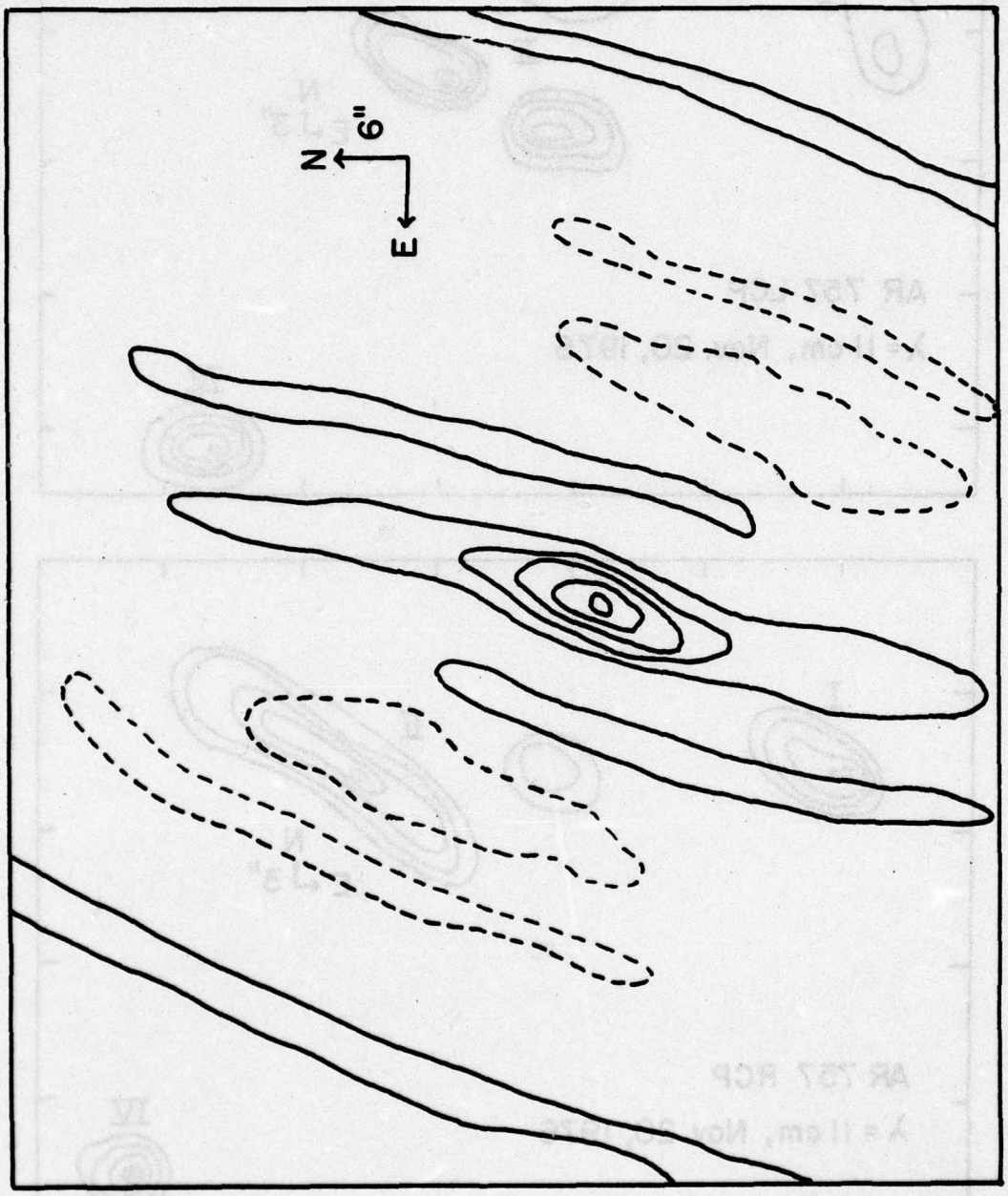

Figure 11. The beam pattern of the three element N.R.A.O. interferometer at 11 cm on November 22, 1976.

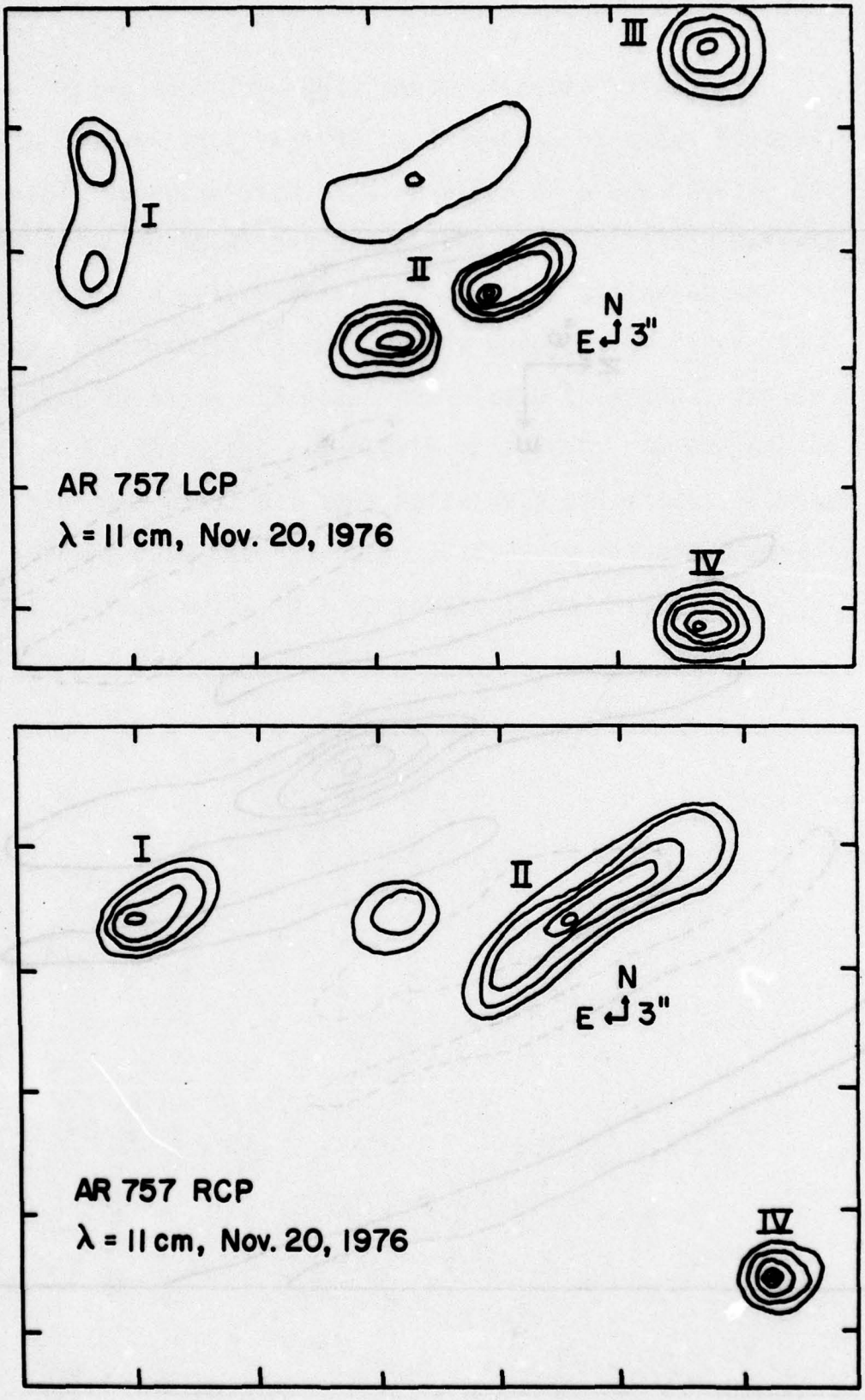

Figure 12. N.R.A.O. Synthesis maps of active region 757 obtained with left (LCP) and right (RCP) circularly polarized radiation at 11 cm wavelength on November 20, 1976.

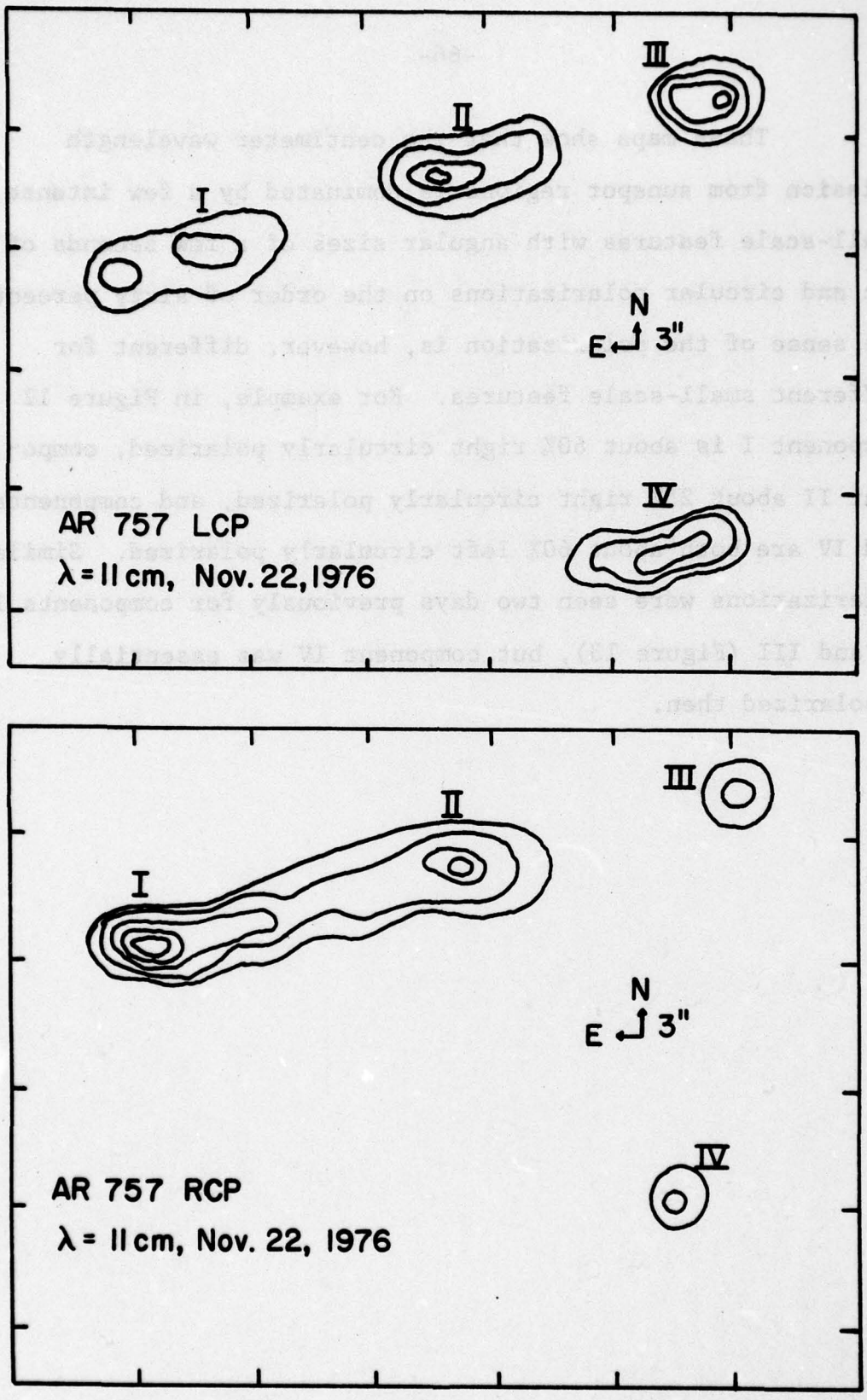

Figure 13. N.R.A.O. synthesis maps of active region 757 obtained with left (LCP) and right (RCP) circularly polarized radiation at 11 cm wavelength on November 22, 1976.

These maps show that the centimeter wavelength emission from sunspot regions is dominated by a few intense, small-scale features with angular sizes of a few seconds of arc and circular polarizations on the order of sixty percent. The sense of the polarization is, however, different for different small-scale features. For example, in Figure 12 component I is about 60% right circularly polarized, component II about 25% right circularly polarized, and components III and IV are both about 60% left circularly polarized. Similar polarizations were seen two days previously for components I, II and III (Figure 13), but component IV was essentially unpolarized then.

3). Synthesis Maps of Solar Active Regions using the Very Large Array (V.L.A.)

The solar active regions 1046 and 1056 were respectively observed with the Very Large Array (V.L.A.) on March 30 and April 1, 1978. During this period no flare activity was reported to any optical or radio observatory. A signal wavelength of 6 cm was used and both the right circularly polarized (RCP) and the left circularly polarized (LCP) signals were sampled every 30 seconds using eleven 25 m diameter paraboloids which provided individual beamwidths of 8.6 minutes of arc. The intermediate frequency signals (bandwidth 12 MHz) for the two different polarizations received at each of eleven antennae were sent to a central location, where they were multiplied together to give the correlated flux for a total of 55 antenna pairs with antenna separations ranging between 70 meters and 10.43 kilometers and effective angular resolutions ranging between one and two hundred seconds of arc.

For each antenna pair the gain, phase and polarization of the correlator outputs were calibrated by observing 3C 84 or CTA 102 for five minutes every twenty minutes. The solar active region was observed during the other fifteen minutes of each twenty-minute period. The levels of the two i.f. signals being fed into each multiplier from each antenna were kept at a fixed value using an automatic level control (a.ℓ.c.) loop in which the sampled signal level controls an attenuator in the final i.f. amplifier. The a.ℓ.c. loop therefore automatically compensates for the variation in

gain magnitude caused by the introduction of an extra i.f. attenuator when observing the Sun. The correlated flux when observing the Sun for each polarization with each antenna pair (m,n) was determined from the equation

$$S_{mn}(\text{sun}) = \frac{R_{mn}(\text{sun})}{R_{mn}(\text{cal})} \frac{[T_{sm}(\text{sun})T_{sn}(\text{sun})]^{\frac{1}{2}}}{[T_{sm}(\text{cal})T_{sn}(\text{cal})]^{\frac{1}{2}}} S_{mn}(\text{cal})\exp[i(\phi_m^*-\phi_m)-i(\phi_n^*-\phi_n)] \tag{12}$$

where R_{mn} denotes the correlated power for one polarization of the antenna pair (m,n).

$$R_{mn}(\text{cal}) = [G_m G_n]^{\frac{1}{2}} \frac{S_{mn}(\text{cal})}{[T_{sm}(\text{cal})\ T_{sn}(\text{cal})]^{\frac{1}{2}}} \exp[i(\phi_m-\phi_n)], \tag{13}$$

where G_m and ϕ_m respectively denote the magnitude and phase of the complex gain of the detection system of antenna, m, the $S_{mn}(\text{cal})$ is the correlated flux when observing the calibration source with one polarization of the antenna pair (m,n), and $T_{sm}(\text{cal})$ denotes the system noise temperature when observing the calibrator source with one polarization of antenna, m. Similarly, when observing the solar active region the correlated power, $R_{mn}(\text{sun})$, for one polarization of the antenna pair (m,n) is given by

$$R_{mn}(\text{sun}) = [G_m^* G_n^*]^{\frac{1}{2}} \frac{S_{mn}(\text{sun})}{[T_{sm}(\text{sun})\ T_{sn}(\text{sun})]^{\frac{1}{2}}} \exp[i(\phi_m^*-\phi_n^*)]. \tag{14}$$

The levels of the two i.f. signals being fed into each multiplier from each antenna were kept at a fixed value using the automatic level control (a.ℓ.c.) loop in which the sampled signal level controls an attenuator in the final i.f. amplifier. This meant that we could assume that the gain magnitudes are the same when observing the calibrator and the sun ($G_m = G_m^*$). The gain phase difference $\phi_m^* - \phi_m$ introduced by the extra i.f. attenuation when observing the Sun was measured for each antenna by observing 3C 84 with the attenuator in and out. The system noise temperatures, $T_{sm}(cal)$, when observing the calibrator were measured for each antenna using a switched noise source whose temperature of 3K was accurately calibrated by observing the Moon. The system noise temperature, $T_{sm}(sun)$, when observing the active region was measured for each antenna by determining the difference in the total power detected when observing the active region and a quiet sun region whose temperature was assumed to be 10^4 K. Even at these high temperatures the front end amplifiers were in their linear, unsaturated regions.

The correlated flux of the calibration source, $S_{mn}(cal)$, was taken to be 49 Jy and 34 Jy, respectively, when observing 3C 84 and CTA 102. The gain and polarization were calibrated by adjusting the digitized output of the correlators to give the same values of $R_{mn}(cal)$ for every baseline pair and both polarizations. This is essentially because the calibrator sources can be assumed to be unpolarized point sources. These instrumental adjustments were also

applied to the solar data. The corrected values of $S_{mn}(sun)$ were then used to construct maps of the solar active regions according to the techniques described in the previous section.

For each polarization of each antenna pair the corrected amplitude, $S_{mn}(sun)$, and the corrected phase $(\phi_m^* - \phi_m) - (\phi_n^* - \phi_n)$ were determined for every 30 seconds of each 15 minute period of solar observation. These amplitudes and phases were taken to be the amplitude and phase of the visibility function, V(u,v). Because corrections for solar rotation and horizontal parallax were incorporated in the computer program which determined the pointing of each antenna, the changing values of the visibility function were then used to measure the brightness distribution of the active region I(x,y), through the fundamental Fourier transform relation given in equation 5.

Figure 14 shows the dirty VLA beam pattern at 6 centimeters constructed from observations during the daylight hours on April 1, 1978 with uniform weighting $w_i = 1$, (cf. equation (11)). The half power width is 1 second of arc x 3 seconds of arc and the highest sidelobe is 14% of the maximum response. One could alter the beam pattern by adjusting the weights. If the outer spacings were more heavily weighted, the beamwidth would become smaller, but at the expense of higher sidelobes. Weighting the inner spacings more heavily would broaden the main beam but decrease the inner sidelobes.

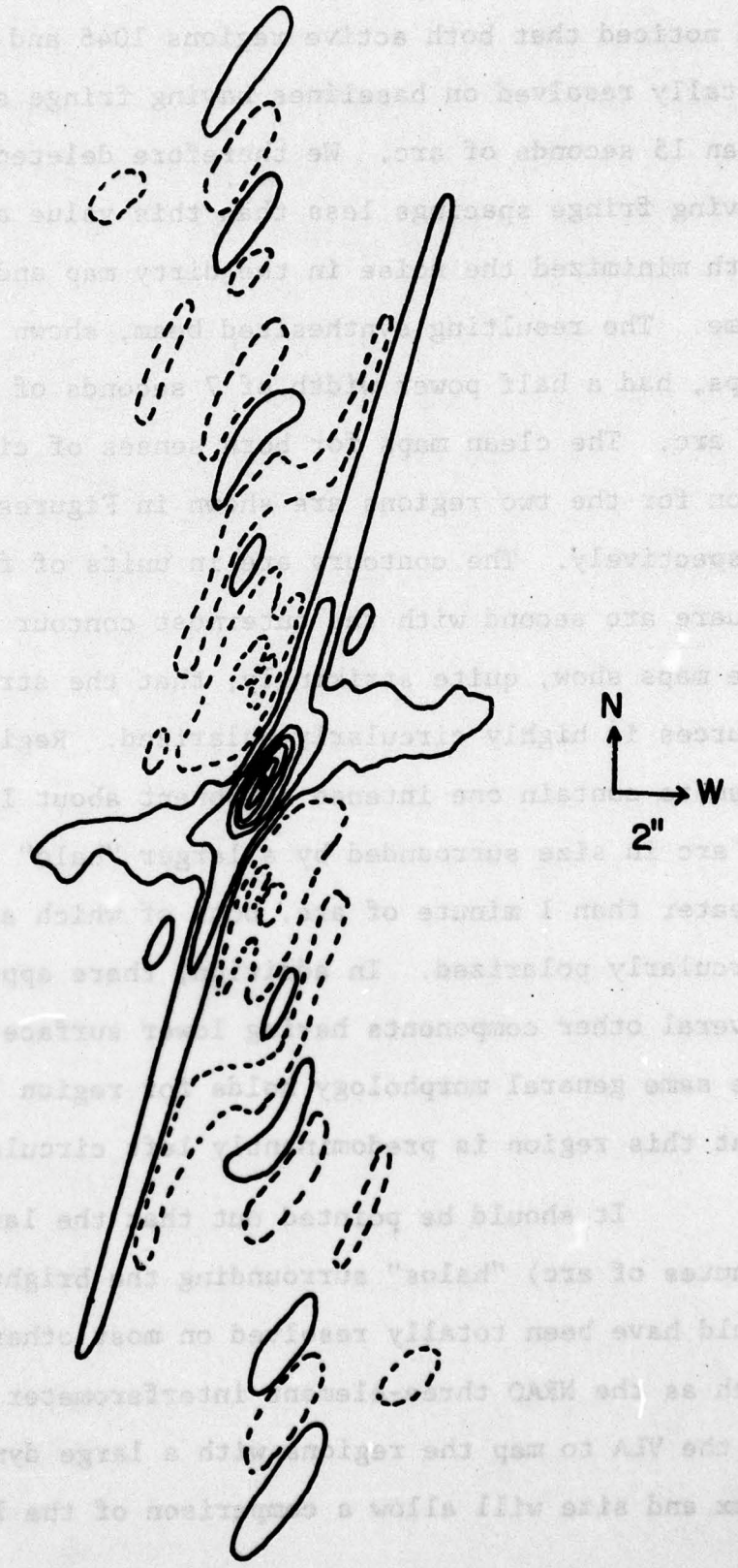

Figure 14. V.L.A. beam pattern at 3 cm wavelength.

After having examined the amplitude and phase data, we noticed that both active regions 1046 and 1056 were about totally resolved on baselines having fringe spacings less than 15 seconds of arc. We therefore deleted those data having fringe spacings less than this value and in so doing both minimized the noise in the dirty map and saved computer time. The resulting synthesized beam, shown on the clean maps, had a half power width of 7 seconds of arc by 20 seconds of arc. The clean maps for both senses of circular polarization for the two regions are shown in Figures 15 and 17, respectively. The contours are in units of flux units per square arc second with the outermost contour drawn at 2. The maps show, quite strikingly, that the structure of both sources is highly circularly polarized. Region 1046 is seen to contain one intense component about 15 to 30 seconds of arc in size surrounded by a larger "halo" with a size greater than 1 minute of arc, both of which are highly right circularly polarized. In addition, there appears to be several other components having lower surface brightnesses. The same general morphology holds for region 1056 except that this region is predominantly left circularly polarized.

It should be pointed out that the larger (2 to 3 minutes of arc) "halos" surrounding the brighter regions would have been totally resolved on most other instruments such as the NRAO three-element interferometer. The ability of the VLA to map the regions with a large dynamic range of flux and size will allow a comparison of the large and

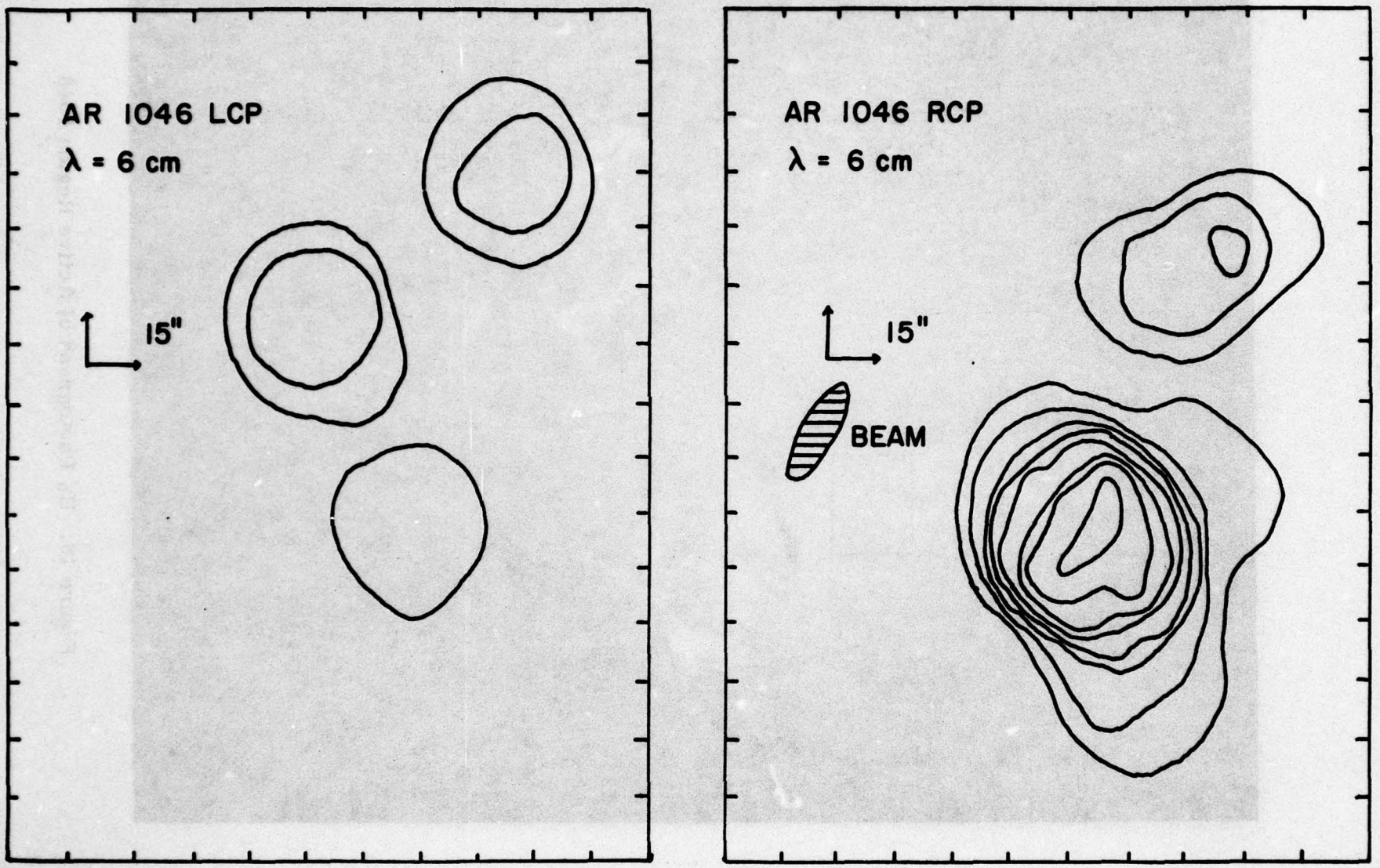

Figure 15. V.L.A. synthesis maps of active region 1046 obtained with left (LCP) and right (RCP) circularly polarized radiation at 3 cm wavelength on March 30, 1978.

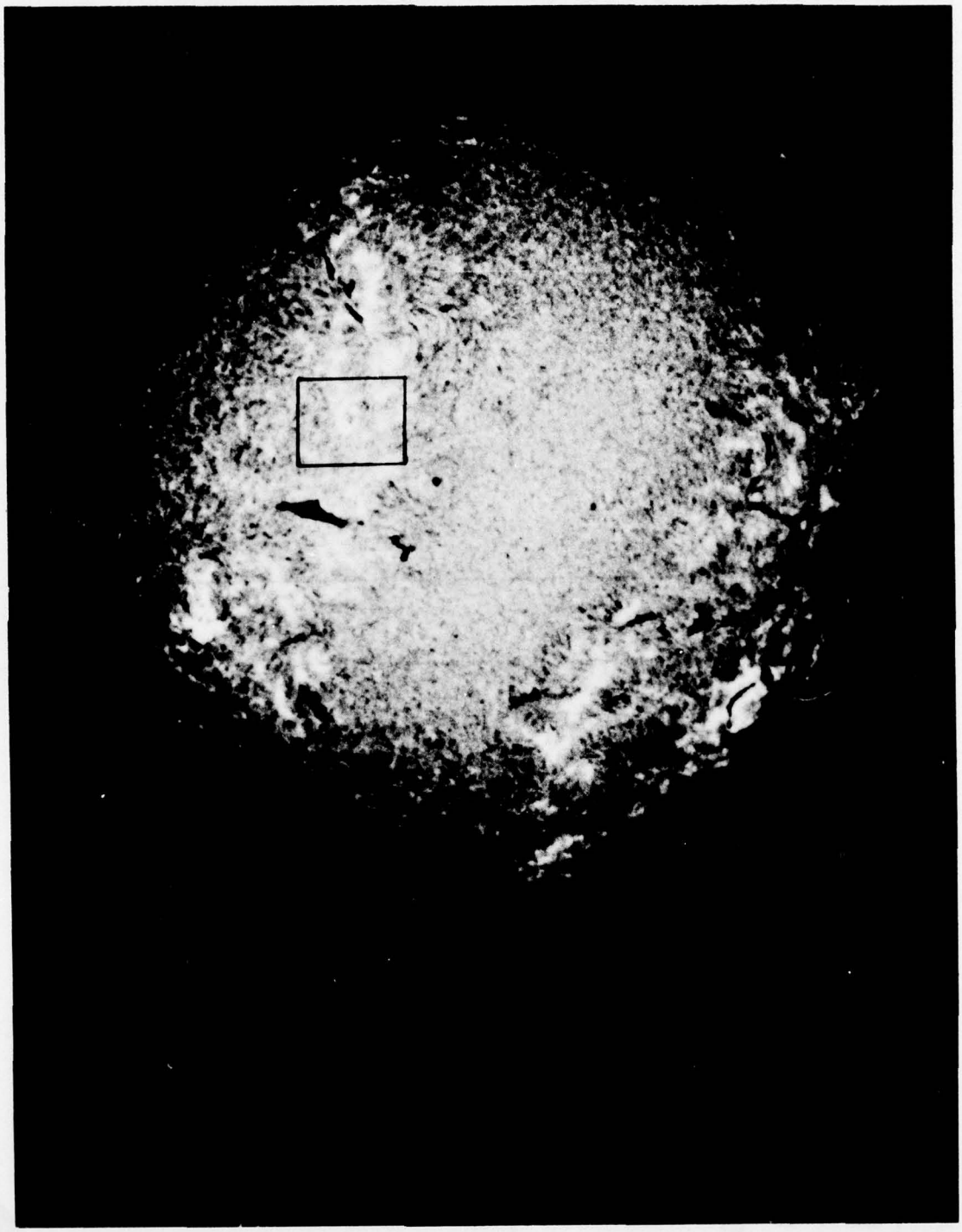

Figure 16. H_α Photograph of Active Region 1046

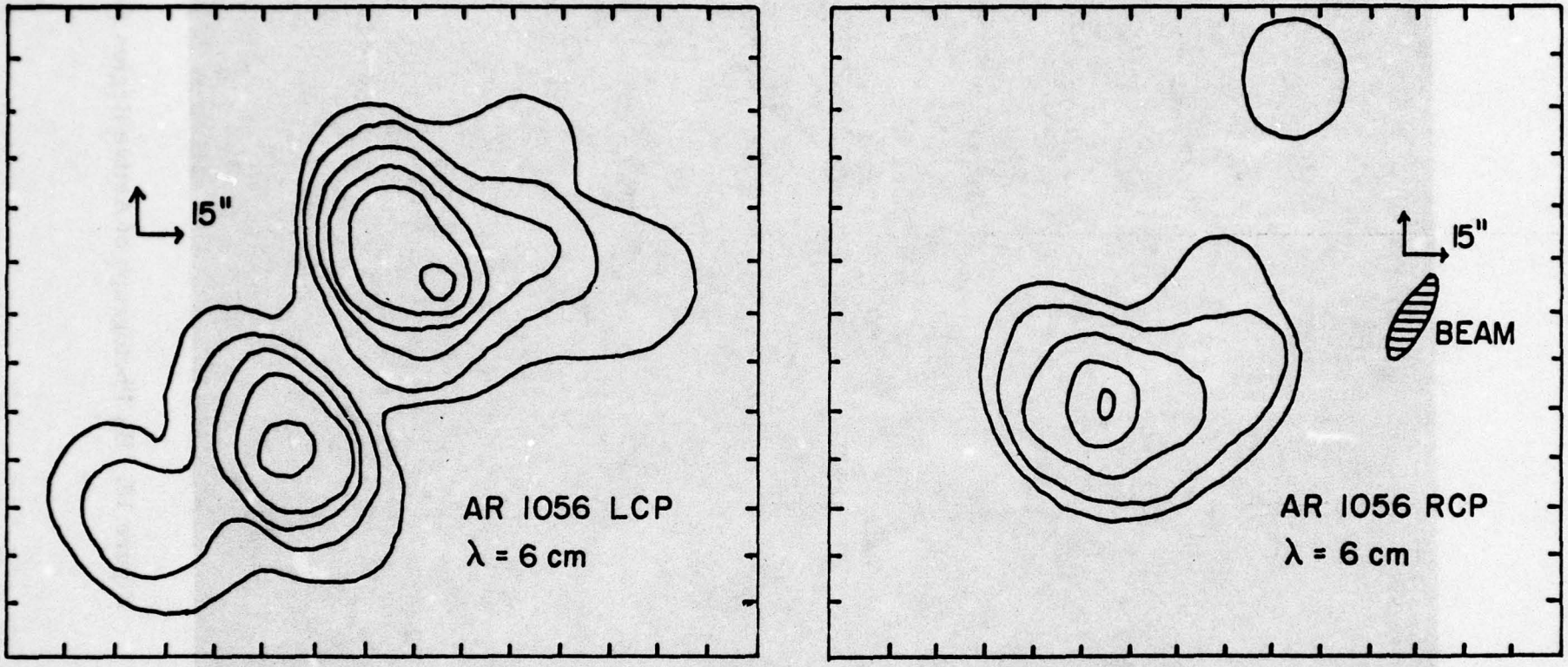

Figure 17. V.L.A. synthesis maps of active region 1056 obtained with left (LCP) and right (RCP) circularly polarized radiation at 3 cm wavelength on April 1, 1978.

Figure 18. H_α Photograph of Active Region 1056

small-scale radio brightness distributions with optically-obtained magnetic field and Hα structures. In fact, for comparison purposes we also show in Figures 16 and 18 the Hα photographs of the same regions taken at the Cal Tech telescopes at the Big Bear solar observatory in California and in Israel.

E. IMPLICATIONS OF RESULTS FOR FUTURE WORK

The research which has been summarized in this report shows that solar active regions emit intense small-scale features at both centimeter and millimeter wavelengths. The small-scale regions are highly circularly polarized with a polarization which remains constant as long as the Sun is not emitting flares. Changes in the circular polarization of the interferometer signal (which are not associated with phase changes) occur immediately before and during solar flare emission. The small-scale sources probably trigger flare emission, and long-term monitoring of these sources should prove the feasibility of using polarization changes for flare prediction. The 8 mm interferometer operated by the Jet Propulsion Laboratory at Table Mountain, California, is an ideal facility for further long-term monitoring of the polarization of the small-scale features. The J.P.L. people are, at their own expense, now installing the required feeds and computer facilities needed to simultaneously monitor right and left hand circularly polarized signals. The large bandwidth, rapid integration time, and the possibility of long-term use for solar observations make the J.P.L. facility ideal for future research along the lines of that reported in this report. In fact, no other interferometric facility in America can be used for the long periods of solar monitoring which are required to obtain a strong statistical record of polarization changes.

The other aspect of the research reported here which warrants further work is the high resolution synthesis maps of solar active regions. Using the Very Large Array (V.L.A.) we have, for the first time, been able to obtain two-dimensional maps of circular polarization with resolutions comparable to those obtainable at optical wavelengths ($\approx$ 1 second of arc). In the future, radio wavelength maps obtained with the V.L.A. at 6 cm should be compared with simultaneous Doppler-Zeeman measurements with large optical telescopes. At 6 cm the VLA covers a field of about 9 minutes of arc by 9 minutes of arc with second of arc resolution. The magnetograms taken with the Tower Telescope at Sacramento Peak can cover a field of about 4 minutes of arc by 4 minutes of arc with second of arc resolution. The magnetograms provide information about the magnetic field structures in the photosphere, whereas measurements of the optical wavelength Hα line can be used to measure motions in the photosphere using the Doppler effect. The polarization features of the V.L.A. maps provide information about the magnetic field in the chromosphere and corona, whereas changes in the spatial distribution of the features can be used to measure motions in these higher levels of the solar atmosphere. A comparison of simultaneous optical wavelength and V.L.A. observations should give information on motions and magnetic field changes which will help decide between the two prevalent solar flare theories--the emerging flux theory and the rearrangement of force-free current fields theory. Moreover, future V.L.A.

observations will provide circular polarization data as a function of time for over 55 different interferometer baselines. This data can be used to test the flare trigger aspect of the small-scale radio sources in active regions.